

SAND REPORT

SAND2002-3870

Unlimited Release

Printed December 2002

Switchable Hydrophobic-Hydrophilic Surfaces

Bruce C. Bunker, Dale L. Huber, Michael S. Kent, Hyun Yim, John G. Curro, Ronald J. Manginell, James G. Kushmerick, Gabriel P. Lopez, and Sergio Mendez

Prepared by
Sandia National Laboratories
Albuquerque, New Mexico 87185 and Livermore, California 94550

Sandia is a multiprogram laboratory operated by Sandia Corporation, a Lockheed Martin Company, for the United States Department of Energy's National Nuclear Security Administration under Contract DE-AC04-94-AL85000.

Approved for public release; further dissemination unlimited.



Issued by Sandia National Laboratories, operated for the United States Department of Energy by Sandia Corporation.

NOTICE: This report was prepared as an account of work sponsored by an agency of the United States Government. Neither the United States Government, nor any agency thereof, nor any of their employees, nor any of their contractors, subcontractors, or their employees, make any warranty, express or implied, or assume any legal liability or responsibility for the accuracy, completeness, or usefulness of any information, apparatus, product, or process disclosed, or represent that its use would not infringe privately owned rights. Reference herein to any specific commercial product, process, or service by trade name, trademark, manufacturer, or otherwise, does not necessarily constitute or imply its endorsement, recommendation, or favoring by the United States Government, any agency thereof, or any of their contractors or subcontractors. The views and opinions expressed herein do not necessarily state or reflect those of the United States Government, any agency thereof, or any of their contractors.

Printed in the United States of America. This report has been reproduced directly from the best available copy.

Available to DOE and DOE contractors from

U.S. Department of Energy
Office of Scientific and Technical Information
P.O. Box 62
Oak Ridge, TN 37831

Telephone: (865)576-8401
Facsimile: (865)576-5728
E-Mail: reports@adonis.osti.gov
Online ordering: <http://www.doe.gov/bridge>

Available to the public from

U.S. Department of Commerce
National Technical Information Service
5285 Port Royal Rd
Springfield, VA 22161

Telephone: (800)553-6847
Facsimile: (703)605-6900
E-Mail: orders@ntis.fedworld.gov
Online order: <http://www.ntis.gov/help/ordermethods.asp?loc=7-4-0#online>



SAND2002-3870
Unlimited Release
Printed December 2002

Switchable Hydrophobic-Hydrophilic Surfaces

Bruce C. Bunker
Biomolecular Materials and Interfaces

Dale L. Huber
Nanostructures and Advanced Materials Chemistry

Michael S. Kent and Hyun Yim
Microsystems Materials, Tribology, and Technology

John G. Curro
Materials and Process Modeling

Ronald P. Manginell
Micro-Total-Analytical Systems

Sandia National Laboratories
P.O. Box 5800
Albuquerque, New Mexico 87185-1413

Gabriel P. Lopez and Sergio Mendez
University of New Mexico
Albuquerque, New Mexico 87106

James G. Kushmerick
Naval Research Laboratory
Washington, DC 20375

Abstract

Tethered films of poly n-isopropylacrylamide (PNIPAM) films have been developed as materials that can be used to switch the chemistry of a surface in response to thermal activation. In water, PNIPAM exhibits a thermally-activated phase transition that is accompanied by significant changes in polymer volume, water contact angle, and protein adsorption characteristics. New synthesis routes have been developed to prepare PNIPAM films via in-situ polymerization on self-assembled monolayers. Swelling transitions in tethered films have been characterized using a wide range of techniques including surface plasmon resonance, attenuated total reflectance infrared spectroscopy, interfacial force microscopy, neutron reflectivity, and theoretical modeling. PNIPAM films have been deployed in integrated microfluidic systems. Switchable PNIPAM films have been investigated for a range of fluidic applications including fluid pumping via surface energy switching and switchable protein traps for pre-concentrating and separating proteins on microfluidic chips.

Acknowledgements

The authors would like to acknowledge the valuable support provided on the interfacial force microscopy experiments by W. L. Smith and J. E. Houston and on infrared experiments by Tim Dunbar.

Contents

	Page
Introduction	6
Synthesis of Switchable Films	7
Characterization of Phase Transitions in Tethered Films	9
Ellipsometry Results	9
Surface Plasmon Resonance Experiments	10
Infrared Results	10
Interfacial Force Microscopy	11
Neutron Reflection	12
Modeling of Polymer Phase Transitions	14
Switching of Surface Chemistry Using PNIPAM	15
Hydrophilic-Hydrophobic Switching	15
Switching of Protein Adsorption	16
Summary	18
Figure Captions	19
References	21

Figures

1. SPR resonance angle vs. temperature for PNIPAM film
2. ATR-FTIR Spectra vs. Temperature for azo-initiated PNIPAM film
3. IFM results vs. temperature for a “polymer brush” PNIPAM film
4. Cloud point data for single PNIPAM chains dissolved in acetone
5. NR data for grafted PNIPAM chains in D₂O and d-acetone
6. NR data for “polymer brush” PNIPAM film in D₂O and d-acetone
7. Spinodal curves for polymer-solvent mixture from PRISM calculations
8. Density profiles from SCF calculations and NR experiments
9. Advancing contact angle vs. temperature for azo-initiated PNIPAM film
10. Advancing contact angle on PNIPAM vs. underlying COOH-CH₃ content
11. Human serum albumin adsorption vs. substrate functionalization
12. UV-visible spectra of myoglobin desorption from PNIPAM films
13. Micro-hotplate device for reversible trapping of proteins
14. UV-visible spectra of PNIPAM film exposed to albumin-myoglobin mix

Introduction

Extensive research is underway to develop microfluidic systems that can separate, purify, analyze, and deliver species such as biomolecules [1-3]. Applications for such systems include controlled drug delivery, proteomics, and the detection and analysis of chemical and biological hazards. The ability to perform chemical and biological analyses on a microchip requires understanding how to transport, separate, and detect species in nanoliter quantities of liquid confined in channels having dimensions of microns. At such small length scales, surface effects play a dominant role. For example, although it is difficult to force liquids through microchannels using pressure, it has been demonstrated that fluids can be transported at cm/sec velocities by manipulating interfacial energies to control whether channel walls attract or repel water [4]. Active control of interfacial energies and exposed chemical functionality could also be used to control selective adsorption for advanced separations and sensors.

Most surfaces currently used in microfluidic systems are passive, having no intrinsic ability to modulate their interactions with fluids or dissolved species such as proteins. Interfacial interactions are often manipulated using self-assembled monolayers (SAMS) [5-7]. Surfaces can be made hydrophobic (or water repellent) by attaching layers to surfaces that are terminated with simple hydrocarbons such as alkane chains. If the alkane chains are terminated with different functional groups, such as hydroxyl groups or carboxylic acids, a hydrophilic (or wettable) surface results. Surface modifications can also control whether surfaces interact with solution species. For example, globular proteins tend to adsorb on hydrocarbon-terminated SAMS [6], while polyethylene oxide (PEO) termination results in an anti-fouling surface [5]. While passive SAMS represent a powerful tool for surface modifications, our interest is in the development of active coatings that can be used to switch surface chemistry in response to “on-chip” stimuli such as heat, light, or an applied voltage. The work described in this report represents the first such system that we have successfully synthesized, characterized, and deployed in a microfluidic system.

The active material forming the basis for our switchable surface is the polymer poly (N-isopropylacrylamide) or PNIPAM [8-12]. In water, this polymer undergoes a phase transition at a lower critical solution temperature of 30-35°C. Below the phase transition temperature (at room temperature), the polymer swells in water. Light scattering studies conducted on polymer chains dissolved in water [11] (or tethered to latex particles [12]) suggest that the swollen polymer occupies over ten times the volume of the dry polymer, with a water content of 90 wt% (50 water molecules per NIPAM monomer). Above the phase transition, the polymer collapses to a state having a much lower volume (around 1.5 times that of dry polymer) and water content (25 wt% or 2 water molecules per PNIPAM monomer). The net volume change in water is around a factor of 8-10 (or 2-3 in any given direction). The swollen polymer is hydrophilic. Above the transition temperature, the polymer surface becomes more hydrophobic. For bulk gels, the contact angle for water can increase from 40° to as high as 90° in going from the swollen to the collapsed state [10]. Since a change in contact angle of only 5-10° is sufficient to pump liquids through microchannels [4], PNIPAM was selected for study as a potential surface modification to promote thermally-programmable active

transport in microfluidic systems. In addition, extensive research on bio-fouling has shown that water-soluble proteins tend to be repelled by hydrophilic surfaces, while such proteins stick to hydrophobic surfaces [13]. Consistent with this trend, it has been demonstrated that PNIPAM-functionalized particles and bulk hydrogels interact more strongly with proteins above the LCST than below it [14,15]. Tethered PNIPAM could potentially activate a surface to grab or release proteins depending on whether the temperature is above or below the transition temperature.

The ability to develop switchable films based on PNIPAM requires that we develop an in-depth understanding of polymeric phase transitions at interfaces. While film functions will be discussed, the major focus of this report is on the materials science issues associated with switchable polymer films. Facets of the materials research to be reported here include: 1) Synthesis of Switchable Films – The phase transition in PNIPAM could be sensitive to parameters such as molecular weight, grafting density, and crosslinking. A range of surface functionalization routes have been developed to vary some of these parameters to determine how material architectures influence film performance characteristics. 2) Characterization of Phase Transitions in Tethered Films – Once films are produced, we need to determine whether the tethered polymer is undergoing the desired phase transition and whether this transition induces desired changes in surface chemistry. Techniques used to characterize the tethered films include ellipsometry, surface plasmon resonance experiments, infrared spectroscopy, contact angle measurements, interfacial force microscopy, and neutron reflectivity. 3) Modeling of Polymer Phase Transitions – Monte Carlo and molecular dynamics simulations have been performed on both dissolved and tethered polymers to understand what factors control the phase transition and to rationalize some of the experimental results. 4) Switching of Surface Chemistry Using PNIPAM – The wetting and protein adsorption behavior of tethered PNIPAM films have been investigated as a function of temperature. Films have been integrated into a micro-hotplate device and incorporated into a microfluidic system. Experiments show that the integrated device can function as a reversible protein trap in microfluidic systems. Below, each facet of the research is described in greater detail.

Synthesis of Switchable Films

PNIPAM films must meet a stringent set of requirements for applications in microfluidic systems. For all applications, we must insure that the tethered polymer is in a configuration that supports a reversible thermally-activated phase transition. The films must also be robust and strongly attached to the surface. However, surface interactions must not be so strong that they inhibit the desired transition. For applications involving the grabbing and release of proteins, the films must have an architecture that allows for rapid and reversible adsorption and desorption kinetics. In bulk gels, protein adsorption tends to be irreversible [8], reflecting steric entrapment of the proteins within a tortuous, high molecular weight network. Due to uncertainties in desired grafting densities, molecular weights, and surface tethering strategies, we investigated a range of different methods for synthesizing thin PNIPAM films.

The simplest method for attaching PNIPAM surface involves grafting pre-polymerized chains to a surface that has been functionalized with a self-assembled

monolayer [16]. In this investigation, we prepared mixed self-assembled monolayers (SAMS) containing a range of relative concentrations of methyl and hydroxyl end groups. Carboxylic acid terminated PNIPAM molecules with molecular weights ranging from 10,000 to 220,000 were then grafted onto the surface hydroxyl groups to form covalent ester linkages. Unfortunately, ellipsometry and neutron reflectivity measurements showed that this grafting method is relatively inefficient, resulting in grafting densities that appear to be too low for meaningful characterization or for practical applications. For grafted chains having molecular weights from 10,000 to 33,000 and –OH fractions in the underlying SAM (available for grafting) ranging from 5% to 80%, no detectable differences in neutron reflectivity data were observed for temperatures ranging from 20°C to 55°C. PNIPAM was barely detected above the SAM background. This means that grafting densities were low and/or that the PNIPAM was swollen to such an extent that it was not detected. The only grafted films that were detectable had a molecular weight of 200,000, and were more likely physisorbed than grafted (see Neutron Reflection Data below).

A more sophisticated method for preparing PNIPAM films involved the in-situ synthesis of PNIPAM on substrates using free radical polymerization of n-isopropylacrylamide (NIPAM) [17,18]. In this route, an azo-initiator that can be activated to produce free radicals was used as the reactive end group on a self-assembled monolayer. The monolayers were tethered to oxide-terminated surfaces using silane coupling agents. On gold surfaces, the azo-initiator was attached to carboxylic acid groups in mixed SAMS with various concentrations of –COOH in a methyl-terminated background. Exposure of the tethered initiator to heat or light promoted cleavage of the azo linkage to create free radicals at the surface. When in contact with a solution containing NIPAM monomer, a surface-initiated free radical chain reaction took place. Films produced by the method (for the case of silane tethered material) were characterized using a combination of ellipsometry, light scattering, infrared spectroscopy, and the interfacial force microscope. Typical films were found to have high single chain molecular weights (around 10^7 as determined by light scattering measurements on detached chains) and low grafting densities (on the order of 4×10^{10} chains/cm² based on ellipsometric film thickness and known molecular weight), yielding chain-chain separations of around 50 nm. Low grafting densities are produced because radicals within the monolayer tend to react with neighboring initiators before they have a chance to react with NIPAM in solution.

In order to produce films with a high graft density, we developed an alternate in-situ polymerization scheme based on the use of a chain-transfer reaction on SAM chains terminated with thiol groups [19]. Here, free radicals are produced in solution using thermal activation of initiators such as azobis(isobutyronitrile) or AIBN and are transferred to the tethered thiols. In contrast to the conventional polymerization process, where chain transfer between surface bound initiators yields a radical and a dead initiator, chain transfer between thiol groups exchanges a radical for a hydrogen atom, yielding a radical and a regenerated thiol. High concentrations of surface radicals can therefore be maintained, allowing for higher grafting densities. With tethered thiols, we can produce films with grafting densities ranging from 10^{11} – 10^{13} chains/cm² (chains are separated by 2-6 nm) with molecular weights ranging from 10^4 – 10^5 . As will be shown below, this high density “polymer brush” configuration is critical for reversible protein traps.

A final synthesis method investigated involved the use of atom transfer radical polymerization (ATRP) from mixed SAM surfaces [20]. This method is a living polymerization process involving a metal complex that supports the existence of free radicals on the end of the growing polymer. The living polymerization method is reported to form polymers with a much narrower polydispersity than can be achieved by other in-situ polymerization methods. Because it is a living polymerization, we can control the polymer film thickness by varying the polymerization time. As with other in-situ methods, the polymer surface coverage can be controlled by varying the composition of the mixed SAM. Although ATRP films have been produced, such films have yet to be characterized. Below, we describe films produced via the other methods, which are denoted as grafted polymers, azo-initiated polymers, and “polymer brushes” (for the chain-transfer films).

Characterization of Phase Transitions in Tethered Films

Ellipsometry Results

For bulk gels, the phase transition in PNIPAM can be monitored by detecting the volume change that accompanies the thermally-induced swelling or deswelling of the material. While detecting the order of magnitude shrinkage in bulk PNIPAM gels (a factor of two in any given direction) is easy, detecting volume changes for a thin (4-8 nm thick) PNIPAM film under water is much more difficult. The “standard” method for measuring film thickness is ellipsometry. In ellipsometry, a plane-polarized light beam is reflected off of a PNIPAM-coated substrate. By measuring the reflection coefficients of the s- and p-polarization components of the reflected beam (which is elliptically polarized), the optical thickness (a convolution of actual thickness and index of refraction) is obtained. If the index of refraction is known, the film thickness can be determined. Assuming that $n = 1.45$ for bulk PNIPAM, we have been able to determine film thicknesses for materials prepared using all of the synthesis techniques described above. Optical thicknesses vary from sample to sample, but typically fall within the range of 4-8 nm. However, it is important to note that the optical thickness is calculated assuming that the PNIPAM films are fully dense. As this assumption is rarely valid, the ellipsometer really provides an estimate of the total mass deposited on the surface. When the grafting density is low, actual film thickness can be much greater than the optical thicknesses indicated by ellipsometry (see below).

While ellipsometry measurement in air can be used to measure films that are only a few nanometers thick, it has been difficult to make in-situ measurements of film thickness under water. This is because the refractive indices of water ($n = 1.33$) and PNIPAM ($n = 1.45$) are similar. To try to observe the lower critical solution temperature for PNIPAM using our ellipsometry equipment, we were forced to perform ex-situ ellipsometry measurements. Samples were immersed in water at various temperatures, removed from solution, quickly blown dry, and placed in the ellipsometer. Using this technique, we found that a typical “polymer brush” film had an effective thickness of 7.5 nm in its swollen state at room temperature. The same film had an effective thickness of 3.5 nm at 50°C, indicating that the tethered PNIPAM film undergoes the expected factor of two change in volume on either side of the phase transition. However, it is hard to

blow-dry samples in such a way as to ensure that all surface water is eliminated without removing water entrapped in the underlying PNIPAM gel. For this reason, all other methods we have used to follow the phase transition have involved in-situ techniques.

Surface Plasmon Resonance Experiments

Surface plasmon resonance (SPR) techniques [21] were used to monitor the phase transition in PNIPAM under water. In SPR, a light beam impinges on the “dry” side of a thin gold layer that is functionalized on the “solution” side with PNIPAM. Most of the light is reflected. However, a small part of the light propagates along the interface between the metal and any dielectrics on the surface as a surface plasmon. The surface plasmon is an evanescent wave that decays exponentially into the dielectric. The fraction of light in the surface plasmon depends on the angle of incidence and the effective optical thickness of the dielectric medium. In the SPR experiment, we monitor the angle of incidence and look for the minimum in the reflected light intensity corresponding to the resonant condition required to produce the surface plasmon. The resonant angle is related to the dielectric constant of the region probed by the evanescent wave. For the PNIPAM films studied here, the effective dielectric constant depends on the dielectric constants of the PNIPAM, the water, and the distribution of the two materials as a function of distance from the interface.

Changes in the SPR resonance angle as a function of temperature are shown in Fig. 1 [22]. The pronounced increase in resonance angle with temperature is consistent with the collapse of a PNIPAM film as it goes through the transition. PNIPAM has a higher dielectric constant than water. Collapse of the film would move the PNIPAM closer to the surface, increasing the amount of higher dielectric constant material close to the interface (in a region where the evanescent wave is more intense), and increasing the resonant angle. To date, we have not been able to quantitatively model the SPR data, as such an analysis requires input regarding the effective dielectric constant as a function of PNIPAM concentration, and simplifying assumptions involving how the PNIPAM is distributed relative to position within the evanescent wave. However, qualitatively the results are consistent with the collapse of a PNIPAM film that is on the order of 100 nm thick in room temperature water. The temperature dependence of the results indicates that while the transition is complete at 32°C (near the expected transition temperature), significant volume changes occur at temperatures well below the transition temperature. (Similar volume changes are apparent in light scattering experiments for single chains [11].) The SPR data indicate that a phase transition does occur in tethered films, but that the transition is not as sharp as the 5-10°C reported for bulk gels.

Infrared Results

Infrared (IR) spectroscopy can be used to detect the vibrations of chemical bonds within thin PNIPAM films. In simple reflectance or transmission modes, IR spectra can be used to identify the chemical nature of the films and to detect the total quantity of material deposited. To monitor the swelling transition, we have used attenuated total reflectance IR (ATR-IR). In ATR-IR, the PNIPAM film is grown on a Si prism. The IR beam enters the prism and is reflected between prism surfaces multiple times. When the

beam encounters the solution side of the interface, the IR beam penetrates the solution with an evanescent wave that exponentially decays with distance from the interface (analogous to the evanescent wave in the SPR technique described above). Although water is an extremely good adsorber of IR radiation, precluding most in-situ IR measurements, in-situ experiments can be performed with ATR because the IR beam interacts with less than a micron-thick layer of water near the surface (the calculated penetration depth into the water is 200 nm for 3600 cm^{-1} light). In contrast to SPR, the intensity of bands associated with PNIPAM vibrations depends only on how much PNIPAM is present as a function of distance from the solution interface. If the PNIPAM film collapses, more PNIPAM is closer to the surface, increasing the intensity of all PNIPAM bands.

ATR-FTIR spectra of high molecular weight PNIPAM films produced via the standard tethered azo initiator are shown in Fig. 2. As expected, the intensities of all PNIPAM bands increase with temperature as the transition temperature is approached, reaching constant values at high temperature. The transition temperature inferred for this film (35°C) is slightly higher than that inferred from the gold-tethered film examined in the SPR experiments. If one assumes that the tethered film collapses by a factor of around three above the transition temperature (consistent with the change in hydrodynamic radius (R_h)) measured for single chains in solution [11]), the observed changes in IR band intensities are consistent with a PNIPAM film that extends around 360 nm from the surface and collapses to around 120 nm.

Similar experiments were conducted on the “polymer brush” films produced via the chain-transfer synthesis route. No phase transition was apparent in the ATR results for this film (the IR intensities did not change appreciably with temperature). We believe that no transition was observed for the brush film because the film was much thinner than the azo-initiated films. For thin films, the swelling transition should not move the PNIPAM a sufficient distance relative to the decaying evanescent wave to cause appreciable intensity changes. However, an alternate explanation is that the tighter packing of chains in the “brush” film is inhibiting the transition. To distinguish between these two possibilities, we probed the thickness of a range of PNIPAM films both below and above the phase transition using the interfacial force microscope.

Interfacial Force Microscopy

The swelling, collapse, and adhesive qualities of tethered PNIPAM films have been monitored as a function of temperature using an interfacial force microscope (IFM). The IFM is a scanning probe system developed by Jack Houston at Sandia National Laboratories to monitor the interactions between functionalized probe tips and substrate surfaces as a function of separation distance with a distance resolution of a few angstroms [23]. The IFM provides force profiles that are similar to those reported for PNIPAM films using the atomic force microscope (AFM) [16] and the surface forces apparatus (SFA) [24]. In experiments reported here, Si or fused silica substrates were functionalized with tethered PNIPAM films. The scanning probe tip was a fused silica rod drawn down and fire polished to produce a tip with a radius that is typically 1-5 μm . Experiments were conducted with bare tips (covered with surface $-\text{OH}$ groups), or with tips coated with octadecyltrichlorosilane ($-\text{CH}_3$ terminated). By moving the IFM tip in a

direction normal to the surface, forces experienced between the tip and the substrate were measured as a function of separation distance. As the tip approached the surface in water, the sequence of events observed for typical tip-substrate interactions was from no interaction at large distances, to detection of through-liquid forces (such as electrical double layer interactions and hydration forces), to measurements of the forces required to deform materials on the tip and substrate as the tip and substrate come into direct contact. The tip position was measured relative to a “zero separation distance” point at which the measured forces are dominated by the mechanical deformation of the Si substrate and the fused silica tip. The IFM tip was also dithered parallel to the substrate to measure frictional forces.

The IFM was used to examine both “polymer brush” films and high molecular weight films produced via azo-initiators. Experiments were performed as a function of temperature (both increasing and decreasing) in deionized water. General features of the resulting force profiles are shown in Fig. 3. At room temperature, a long range repulsive force was detected as the tip approached the “polymer brush” film at a distance of around 100 nm. The repulsion was similar regardless of tip functionalization, indicating that it was not due to the presence of an electrical double layer. The repulsion did not depend on tip speed, indicating that it was not a repulsive hydration force arising from the presence of an ordered water layer near the surface. On the azo-initiated PNIPAM film with a molecular weight of 10^7 , the repulsion was detected at a distance of 320 nm, which corresponds almost exactly with the hydrodynamic radius of single PNIPAM chains at room temperature [11]. We believe that the observed repulsion is due to physical contact between the tip and hydrated PNIPAM chains on the substrate and subsequent deformation of the PNIPAM film by the tip. As the temperature was increased, there was no apparent change in this repulsion until the temperature reached between 25-28.5°C. At this point, there was an abrupt change in the repulsion, which collapsed toward the surface by about a factor of two and became stronger (as evidenced by a steeper slope). However, after the abrupt change, the repulsion stayed roughly constant up to at least 50°C. We believe that the collapse of the repulsive force reflects the collapse of the PNIPAM film.

As the tip is retracted from the surface above the transition temperature, the PNIPAM film is attracted to the tip (the measured force drops below zero), indicating that the PNIPAM is undergoing adhesive interactions with materials it comes into contact with. However, these adhesive interactions disappear below the transition temperature, and the PNIPAM surface repels all functionalized tips on retraction as well as on approach. All of these findings are consistent with force profiles obtained elsewhere on PNIPAM films using an atomic force microscope [16] and a surfaces forces apparatus [24]. The IFM experiments suggest that materials such as dissolved proteins should be repelled by PNIPAM surfaces in water below the transition temperature, but can stick to the PNIPAM above the transition. The IFM force profiles not only indicate that “polymer brush” films undergo a sharp phase transition, but that the transition might be useful for applications such as a reversible protein trap.

Neutron Reflection

A final technique investigated for observing the phase transition in thin PNIPAM films was neutron reflection. Neutron reflectivity (NR) is a technique that can provide density profiles for thin polymer films in the presence of deuterated solvents [25]. The solvents investigated in the NR experiments were D₂O and d-acetone. Acetone is of interest because experimental cloud point data (Fig. 4) show that PNIPAM exhibits an upper critical solution temperature (UCST) in acetone. In contrast to its behavior in water, PNIPAM films should be insoluble and collapsed below the phase transition temperature in acetone, and swollen (or soluble) above the transition temperature. However, since the transition temperature in acetone is well below room temperature, PNIPAM should be highly swollen in acetone at room temperature just as it is in ambient water.

NR was able to detect the presence of PNIPAM for both the highest molecular weight (220,000) grafted samples as well as for “polymer brush” films (Fig. 5,6) [26]. In acetone (at 20°C), both films exhibited a smoothly decaying single profile. The apparent volume fractions occupied by PNIPAM at the immediate surface were 0.28 and 0.39 for the grafted and polymer brush films, respectively. The effective thicknesses for the PNIPAM films (position where the density drops to half of its value at the immediate surface) were 10 nm and 7.5 nm for the grafted and polymer brush films, respectively. For the polymer brush film, the NR thickness determined in acetone is an order of magnitude less than the thickness inferred from the IFM results described above. The NR data suggest that although PNIPAM films swell in acetone, the extent of swelling is less than that reported for PNIPAM in cold water (swollen volume/dry volume = 2.6 and 1.5 for the grafted and brush films, respectively, compared to 10 for PNIPAM dissolved in water). The limited swelling may reflect the fact that attachment to the surface is inhibiting the ability of PNIPAM to expand, particularly at the high chain densities expected for the polymer brush film. The swelling may also be influenced by attractive interactions between the polymer segments and the surface, particularly for the grafted chains. Model fits to the NR density profiles for PNIPAM in acetone suggest that such surface interactions are significant (see Modeling of Polymer Phase Transitions).

Although NR data have been obtained in water both below and above the transition temperature (at 20°C and 55°C), the density profiles inferred from the NR data are not consistent with any experimental or modeling results obtained on this project or reported in the literature (including the NR results in acetone). In water, bilayer profiles were required to fit the NR data for both film types. The NR results suggest that there is a thin layer of high PNIPAM concentration next to the immediate surface. Above this layer is a second layer of much lower concentration that extends well into the water. Although each layer exhibits reversible changes with temperature, the changes are minor. Neither layer exhibits density changes that are consistent with a robust phase transition. The NR data suggest that for both grafted and polymer brush films, a relatively dense layer of PNIPAM exists at the immediate surface that does not swell in water at any temperature. While polymerization from the surface in the “polymer brush” film could generate chain densities near the surface that would be sufficient to inhibit swelling, it is unclear why this dense layer should be seen in room temperature water but not in room temperature acetone. (Perhaps chain segments are strongly physisorbed to the surface in water but not in acetone.) The presence of a diffuse outer layer of PNIPAM could account for the discrepancy in apparent film thickness between the NR and IFM results.

For the “polymer brush” film, the expected polydispersity in the tethered film could allow for the presence of a less densely-packed outer layer whose swelling and collapse is apparent in the IFM data. However, it is unclear why there is no NR evidence for a robust phase transition in this outer layer unless the volume fraction in the outer zone is simply too low to generate meaningful NR results.

Modeling of Polymer Phase Transitions

While the experiments described above indicate that tethered PNIPAM exhibits a lower critical solution temperature similar to that observed in bulk solutions, the various techniques yield different results regarding details such as the transition temperature, the sharpness of the transition, and the volume fraction occupied by PNIPAM in the swollen and collapsed phases. To develop further insight regarding the nature of polymer swelling transitions, we have developed computational models that allow us to study the phase behavior of bulk polymers as well as tethered chains immersed in a solvent.

The first phase of the modeling effort involved simulating the behavior of simple polymers immersed in a simple solvent [27]. In the model, the polymer was represented by “strings of pearls” consisting of identical spherical units. The solvent was represented using isolated spheres having the same diameter as the “monomers” in the polymer chain. All sites were allowed to interact with each other via repulsive Lennard-Jones interactions within a self-consistent polymer reference interaction site model, or PRISM, theory. PRISM is a liquid state theory in which generalized Ornstein-Zernike integral equations are solved numerically in a self-consistent manner to obtain the chain intermolecular structure and intermolecular radial distribution functions. With PRISM, we were able to explicitly include discrete solvent molecules. By using the random phase approximation together with direct correlation functions (the output of PRISM theory), we were able to estimate the phase diagram for a given polymer solution.

To date, PRISM theory has been used to estimate the spinodal curves for “normal” polymers in “normal” solvents (representative of PNIPAM in acetone). For the case where solvent-polymer interactions (ϵ_{sp}) are much less attractive than polymer-polymer (ϵ_{pp}) and solvent-solvent interactions (ϵ_{ss}) ($\epsilon_{ss} = \epsilon_{pp}$ in the calculations), polymer-solvent mixtures exhibit an upper critical solution temperature (UCST) as predicted by Flory-Huggins theory. The polymer and solvent are immiscible at low temperature, with swelling or dissolution occurring above the spinodal decomposition temperature. The transition temperature T_s increases with the strength of polymer-polymer attraction and with the molecular weight of the polymer (both of which make the polymer less soluble). T_s goes through a maximum as the mole fraction of polymer is increased, with the maximum moving to lower polymer mole fractions as the molecular weight increases. All of the above phenomena are in qualitative agreement with Flory-Huggins theory. However, PRISM calculations suggest that similar behavior should be observed even when polymer-solvent interactions become significant. Fig. 7 shows the phase diagram calculated for the case where $\epsilon = \epsilon_{sp} = \epsilon_{ss} = \epsilon_{pp}$. Here, Flory-Huggins theory would predict that such a mixture would be completely miscible. The fact that UCST behavior is still observed is driven by nonrandom mixing and compressibility effects that are included in PRISM, but are neglected in Flory Huggins theory (which treats the solvent as a continuum rather than as discrete molecules).

Tethered polymer brushes were modeled with self-consistent field (SCF) theory [28]. Here we simplified the problem of many tethered polymer chains surrounded by solvent molecules to a problem of a single polymer that interacts with the surface through a potential field that must be solved for in a self-consistent manner with site volume fraction profiles. Our approach for modeling the phase behavior of the tethered brushes was to determine the temperature-dependent χ interaction parameter with Flory-Huggins theory. The χ parameter was extracted from experimental cloud point curves for polymer solutions of interest (Fig. 4). With SCF theory, we were able to generate polymer site density profiles that could be compared directly to the experimental neutron reflection data (Fig. 8). In the calculated plot, the only parameter that was adjusted was the interaction parameter between the polymer sites and the surface. The experimental and calculated curves are in agreement except for a pronounced feature at low wave vector ($q = 0.02 \text{ \AA}^{-1}$). This feature disappears when one accounts for the polydispersity of the grafted chains. Density profiles predicted by SCF theory are also in good agreement with the profiles extracted from NR data. The SCF results indicate that it should now be possible to model phase transitions for tethered polymers as the interactions between critical components (the polymer, solvent, and surface) are varied, aiding in the development of responsive films.

Switching of Surface Chemistry Using PNIPAM

Although the volume change associated with the phase transition in PNIPAM could be of use for physical actuation of valve in microfluidic devices, the fluidic applications of interest in this proposal rely on the use of the phase transition to modify the chemistry of the surface. Below, we describe experiments that have been conducted to determine how the transition can be used to modify interfacial energies and interactions with solution species such as proteins.

Hydrophilic-Hydrophobic Switching - Contact Angle Measurements

Water contact angle measurements provide a convenient measure of interfacial energies as well as providing direct information regarding how hydrophilic or hydrophobic a surface is. Water contact angle measurements provide a direct measure of the forces that can be exploited for moving droplets in microfluidic systems based on active switching of interfacial energies with a tethered PNIPAM film. The expression relating the velocity at which gradients in interfacial energy can be used to pump fluids through microchannels is given by [4]:

$$v = \text{droplet velocity} = (h/6\mu L[(\sigma \cos\theta)_a - (\sigma \cos\theta)_r])$$

where h is the height of the fluid channel, μ is the viscosity of the droplet, L is the length of the droplet, σ is the surface tension of the liquid, θ is the solid-liquid contact angle, and the subscripts a and r refer to the advancing and trailing sides of the droplet. Eq. 1 suggests that for water, a difference in contact angle of as little as 10° should be sufficient to move droplets at sufficient velocities to be of interest for microfluidic systems.

Advancing contact angles on a pure azo-initiated PNIPAM film (Fig. 9) show that the thermally-activated phase transition induces pronounced changes in interfacial energies. For tethered films, the contact angle typically increases by around 25° (from 60° to 85°) as the temperature is increased from room temperature to above the transition temperature. The transition temperature inferred from the contact angle data is around 35°C . Both the transition temperature and magnitude of the contact angle change are consistent with values reported for PNIPAM films in the literature [10].

Not only can PNIPAM be used to switch contact angles, it can be used as a component in mixed monolayers to tune the contact angle [29]. In mixed-monolayers containing CH_3 and COOH only (no PNIPAM), the advancing contact angle can be tuned from around 115° (pure CH_3) down to around 30° (pure COOH). Once PNIPAM is grown on mixed films by attaching azo-initiators to the COOH fraction, the contact angle measured for the “hydrophobic” state at 45°C exhibits a similar trend with CH_3 mole fraction (Fig. 10). However, in the presence of PNIPAM, the contact angle can be switched from the “baseline” value to a value that is around 20° lower by lowering the temperature to below the transition temperature (to 25°C) regardless of the COOH mole fraction. The ability to both tune and modulate contact angles could be important for a wide range of fluidic applications.

The significant changes in advancing contact angle observed for both pure and mixed monolayers containing PNIPAM were initially promising with regard to applications involving the transport of liquids by switching interfacial energies. Unfortunately, all PNIPAM films exhibit a large hysteresis between the advancing (measured as the film is pushed into water) and receding (measured as the wet film is retracted from water) contact angles. For a pure PNIPAM film, measured values for the receding contact angle are low (around 40°) and are independent of temperature. As the driving force for propelling fluids in microchannels is based on the difference between the advancing contact angle on the “hydrophilic” leading edge of a droplet and the receding contact angle on the “hydrophobic” trailing edge, this contact angle hysteresis represents a serious concern for fluidics applications. Our speculation is that this hysteresis arises because there is a low barrier to rotation for functional groups at the end of the PNIPAM chains adjacent to the solution. In air, hydrophobic isopropyl groups are present at the surface, resulting in a surface that is relatively hydrophobic. However, in water the lowest energy configuration is one in which more polar functional groups (such as carbonyl groups) rotate to face the solution, while the isopropyl groups move away from the immediate interface, dramatically lowering the contact angle. Strategies for minimizing the hysteresis (particularly above the transition temperature) could involve the introduction of chain-end modifications (such as modified alkenes) to minimize free rotations at chain ends. Such modifications were not pursued because it was discovered that unmodified PNIPAM films exhibit the ability to switch interactions with solution species such as proteins, opening up a completely new range of applications for PNIPAM in fluidic devices.

Switching of Protein Adsorption

Extensive research on biofouling has shown that water soluble proteins tend to be repelled by hydrophilic surfaces, while such proteins stick to hydrophobic surfaces [7].

Consistent with this trend, it has been demonstrated that PNIPAM-functionalized particles and bulk hydrogels interact more strongly with proteins above the LCST than below it [14,15]. We performed a series of protein adsorption experiments on our tethered PNIPAM films that have led to the development of an integrated device which functions as a reversible protein trap [30]. The protein adsorption experiments and the protein trap are described below.

The changes in interactions between proteins and surfaces functionalized with PNIPAM can be quite dramatic, as indicated by the ellipsometry data shown in Fig. 11. At room temperature, the adsorption of large globular proteins such as human serum albumin (HSA) is negligible on a tethered PNIPAM film. The antifouling character of the film is comparable to that of polyethylene oxide (PEO) SAMs [5]. Above the transition temperature, HSA adsorption is extensive. Complete protein monolayers form at rates comparable to those seen on hydrocarbon-terminated octadecyltrichlorosilane (ODTS) functionalized surfaces. For large globular proteins such as HSA, complete desorption of the protein is observed on cooling the PNIPAM to room temperature.

More detailed protein adsorption experiments have been conducted on proteins such as myoglobin containing a heme group that can be monitored using UV-visible spectroscopy [31]. UV visible spectra of myoglobin provide a quantitative measure of adsorbed protein concentrations and indicate whether the protein has denatured on the surface. For myoglobin, denaturation results in a characteristic blue shift of the Soret peak from its native position at 408 nm to 395 nm for strongly denatured protein. Fig. 12 shows a series of spectra taken during the desorption of myoglobin from two types of PNIPAM films: an azo-initiated film with a low grafting density and high molecular weight, and a “polymer brush” film with a higher grafting density and lower molecular weight. While both films adsorb a monolayer of myoglobin above the transition temperature, a fraction of a monolayer (up to 25%) is retained on the low graft-density film on cooling. The UV visible spectra reveal that the irreversibly adsorbed fraction consists of denatured myoglobin. Studies on other proteins suggest that the fraction of irreversibly adsorbed protein varies inversely with protein size (< 1% for HSA (14 x 4 x 4 nm dimensions), 10-15% for hemoglobin (6.5 x 5.5 x 5.0 nm), and 15-25% for myoglobin (4.4 x 4.4 x 2.5 nm). Our interpretation of these results is that for the low graft-density films, collapse of the tethered chains above the transition temperature opens up bare patches that are on the order of 5-6 nm in diameter. Proteins that are smaller than these holes can gain access to the underlying substrate, where they denature and stick. In contrast, UV-visible spectra show that myoglobin does not denature on the more tightly packed “polymer brush” films, resulting in completely reversible adsorption. Use of the “polymer brush” configuration is critical to the performance of reversible protein traps.

“Polymer brush” PNIPAM films have been incorporated into a micro “hotplate” device (Fig. 13) that allows for rapid heating and cooling of protein solutions in small volumes. The device consists of an array of gold heater lines deposited on a thin, freestanding membrane of silicon nitride to provide for thermal insulation from the surrounding Si wafer frame. The membrane and heater lines are covered with a thin layer of silica which provides electrical insulation from the fluid as well as a substrate for the PNIPAM SAM. Fluidic channels are defined above the hot plate with glass spacers and silicon adhesive. Fluids are delivered to the system using capillary tubes connected to syringe pumps. The response characteristics of the fluidics device containing PNIPAM

films have been tested by monitoring the adsorption and desorption of fluorescein-labeled myoglobin from static solutions using fluorescence microscopy. Fig. 13 shows successive video images taken for a line that was heated above the transition temperature and then rinsed with a protein-free buffer solution. Fluorescence microscopy reveals that a layer of myoglobin forms only above the heated line. The remainder of the surface, which is covered with room temperature PNIPAM, is completely non-fouling. An image taken less than one second after the heater line is turned off shows a plume of myoglobin desorbing from the surface. (The fluorescence intensity of the desorbing plume is higher than the intensity of the initial heated line because the fluorophores do not quench each other to the extent that they do in a densely packed monolayer.) For myoglobin, the desorption process is complete in a few seconds. However, desorption kinetics are protein dependent, with larger proteins such as HSA requiring longer times to desorb and diffuse away from the cooling line.

While the protein trap described above could be used as a reversible on-chip protein preconcentrator, it may be possible to exploit the kinetics of competitive adsorption and desorption to perform on-chip separations. For example, UV-visible spectra obtained on hot PNIPAM films in contact with myoglobin-albumin mixtures (Fig. 14) show that the smaller myoglobin forms a monolayer on the surface in around 30 seconds. However, with longer exposure times (< 10 minutes), the larger HSA eventually displaces the myoglobin to form a relatively pure HSA monolayer. Such results are consistent with literature studies of competitive adsorption on passive surfaces [32]. By programming an array of heater lines and controlling contact times and flow rates, it should be possible to selectively grab either myoglobin or albumin from protein mixtures. Use of an array of such devices could provide a mechanism for performing tasks such as extracting relatively dilute populations of cytokines (small cell-signalling proteins) from albumin-rich serum as part of a rapid screening test to identify persons who have been exposed to chem-bio warfare agents. The protein trap could also see use in a wide range of other applications including on-command drug delivery, proteomics, and (when used to adsorb antibody monolayers) highly selective separations of biomolecules.

Summary

Tethered films of the polymer poly n-isopropylacrylamide (PNIPAM) were synthesized and characterized for their potential as thermally-switchable coatings in microfluidic systems. With PNIPAM films, switching of surface chemistry is achieved by virtue of a thermally-activated swelling transition in water which occurs at a lower critical solution temperature of 30-35°C. A wide range of techniques, including ellipsometry, surface plasmon resonance, attenuated total reflectance infrared spectroscopy, and interfacial force microscopy, all indicate that the swelling transition occurs regardless of the grafting density and molecular weight of the polymer chains in the film. Desired chemical changes, including switching of the water contact angle and the reversible adsorption and desorption of proteins, also indicate that tethered PNIPAM films exhibit the desired phase transition.

Each of the above techniques is sensitive to a different aspect of the phase transition. While experimental results were in qualitative agreement, quantitative values

that characterize the transition varied from technique to technique and from sample to sample. Values for the transition temperature ranged from 27°C (IFM results on the polymer brush) to over 35°C (for water contact angle changes on azo-initiated films). The extent of swelling inferred from different measurements ranged from a negligible change in volume (from neutron reflectivity) to almost a factor of three (from ATR-FTIR). Some techniques (such as IFM) indicate that the transition is sharp, while other methods (such as SPR) suggest that the transition occurs over almost 20°C. Unfortunately, most of the techniques used to characterize films had their own unique requirements that dictated different synthesis methods and substrates, precluding head-to-head technique comparisons. Such comparisons will be required to allow us to establish whether the observed differences are due to the materials themselves (grafting density, molecular weight, and substrate interactions), experimental artifacts, or differences in a range of physical phenomena associated with the transition. (For example, substantial contact angle changes may not occur until most of the water is expelled from the PNIPAM, resulting in a higher apparent transition temperature for the contact angle measurement.) Further development of the phase transition models initiated on this project may elucidate the critical parameters that influence the diverse properties measured by the available characterization methods.

Specific applications of tethered PNIPAM films that were investigated included the use of hydrophilic-hydrophobic switching to pump liquids through microchannels and the reversible trapping of proteins for on-chip protein separations. Preliminary experiments indicated that the pumping of liquids may not be feasible due to the large hysteresis observed between the advancing and receding contact angles on PNIPAM in water. However, PNIPAM has been successfully incorporated into a micro-hotplate device that can rapidly adsorb and desorb protein monolayers. For the protein trap application, protein adsorption studies indicate that a “polymer brush” configuration (high grafting density plus low molecular weight) is necessary to prevent irreversible denaturing and adsorption of small proteins. The “polymer brush” micro-hotplate combination is currently being explored for applications in “on-chip” systems for preconcentrating and separating proteins.

Figures

1. Plot of resonance angle vs. temperature from SPR measurements on a PNIPAM film prepared by atom transfer radical polymerization on a mixed COOH-, CH₃-terminated thiolate SAM.
2. a) ATR-FTIR spectra obtained for an azo-initiated PNIPAM film on Si as a function of temperature. b) change in absorbance in both C-H stretch and amide I vibrational modes of PNIPAM vs. temperature showing phase transition near 35°C.
3. IFM data obtained on a “polymer brush” PNIPAM film on Si vs. temperature. Left – As the tip approaches the surface, the interaction with PNIPAM is purely

- repulsive, with the repulsion collapsing into the surface at 26.5°C. Right – Above the transition temperature, adhesive interactions are observed on tip retraction (the region from 200-400 angstroms where the observed force is negative).
4. Left - Cloud point data for PNIPAM chains (molecular weight = 249,000) dissolved in acetone. Right – Chi parameter extracted from the cloud point data using Flory-Huggins Theory.
 5. Left – Neutron reflection data for “grafted” PNIPAM chains (molecular weight = 220,000) in D₂O and d-acetone. Right – PNIPAM density profiles extracted from the NR data.
 6. Left – NR data for “polymer brush” PNIPAM films in D₂O and acetone. Right – PNIPAM density profiles extracted from the NR data.
 7. Spinodal curves generated with an output of PRISM calculations for polymer solutions as a function of the number of monomers (N) in the chain.
 8. Comparison of experimental NR data for grafted PNIPAM (molecular weight = 220,000)(circles) and NR curves calculated using SCF theory density profiles. Inset – Comparison of experimental and calculated density profiles.
 9. Advancing contact angle vs. temperature for azo-initiated PNIPAM film showing phase transition near 35°C.
 10. Advancing water contact angles on mixed CH₃-COOH SAMS on which PNIPAM was polymerized vs. COOH mole fraction above (at 45°C, squares) and below (25°C, diamonds) the PNIPAM transition temperature.
 11. Thickness of human serum albumin film on different substrates as a function of time as measured via ellipsometry.
 12. UV-visible spectra of myoglobin desorbing from PNIPAM films. Left – Desorption from a high molecular weight, low grafting film produced via azo-initiation showing the denaturing and irreversible adsorption of a fraction of the adsorbed myoglobin. Right – No denaturing is observed on the “polymer brush” film produced via chain transfer polymerization.

13. a) Cross-section schematic of the micro-hotplate device showing the relative locations of the Si substrate, the Si₃N₄ membrane, the gold heater lines, the PNIPAM film, and the fluidics. b) Left – photomicrograph of the top of the hotplate (the silicon nitride membrane (bright region in the center) is 200 nm wide. Right – Calculated thermal profiles around a single heated line. c) Fluorescence microscope images of PNIPAM desorbing from a single hot line as a function of time after the hot line is turned off.
14. UV-visible spectra of protein films adsorbed on PNIPAM above its transition temperature. Protein solutions containing both myoglobin and human serum albumin result in initial adsorption of myoglobin (red curve) followed by the displacement of myoglobin by albumin at long contact times (green curve).

References

1. G. M. Whitesides and A. D. Strook, *Phys. Today*, 54, 42 (2001)
2. D. Figeys and D. Pinto, *Electrophoresis*, 22, 208 (2001)
3. J. C. McDonald, et al., *Electrophoresis*, 21, 27 (2000)
4. M. A. Burns, et al., *Proc. Nat. Acad. Sci.*, 93, 5556 (1996)
5. P. Harder, M. Grunze, R. Dahint, G. M. Whitesides, and P. E. Laibinis, *J. Phys. Chem. B*, 102, 426 (1998)
6. E. Ostuni, L. Yan, and G. M. Whitesides, *Colloid Surf. B, Biointerfaces*, 15, 3 (1999)
7. K. L. Prime and G. M. Whitesides, *Science*, 252, 1164 (1991)
8. R. Pelton, *Adv. Colloid Interface Sci.*, 85, 1 (2000)
9. Y. G. Takei, et al., *Macromolecules*, 27, 6163, (1994)
10. J. Zhang, R. Pelton, and Y. Deng, *Langmuir*, 11, 2301 (1995)
11. C. Wu and S. Zhou, *Macromolecules*, 28, 8381 (1995)
12. X. Wang, X. Qiu, and C. Wu, *Macromolecules*, 31, 2972 (1998)
13. S. Oscarsson, *J. Chromatography B*, 699, 117 (1997)
14. H. Kanazawa, et al., *Anal. Chem.*, 68, 100 (1996)
15. H. Lakhari, et al., *Biochim. Biophys. Acta General Subjects*, 1379, 303 (1998)
16. S. Kidoaki, S. Ohya, Y. Nakayama, and T. Matsuda, *Langmuir*, 17, 2402 (2001)
17. L. Liang, X. D. Feng, J. Liu, P. C. Rieke, and G. E. Fryzell, *Macromolecules*, 31, 7845 (1998)
18. L. K. Ista, S. Mendez, V. H. Perez-Luna, and G. P. Lopez, *Langmuir*, 17, 2552 (2001)
19. A. Revillon, and D. Leroux, *React. Funct. Polymers*, 26, 105 (1995)
20. T. E. Patten and K. Matyjaszewski, *Acc. Chem. Res.*, 32, 895 (1999)
21. L. S. Jung, C. T. Campbell, T. M. Chinowsky, M. N. Mar, and S. S. Yee, *Langmuir*, 14, 5636 (1998)
22. B. Subramanian, S. Mendez, S. Balamurugan, M. O. O'Brien, and G. P. Lopez, manuscript in preparation

23. S. A. Joyce and J. E. Houston, *Rev. Scientific Instrum.*, 62, 710 (1991)
24. F. –J. Schmitt, C. Park, J. Simon, H. Ringsdorf, and J. Israelachvili, *Langmuir*, 14, 2838 (1998)
25. M. S. Kent, *Macromol. Rapid Commun.*, 21, 243 (2000)
26. H. Yim, M. S. Kent, D. L. Huber, S. Satija, J. Majewski, and G. S. Smith, submitted to *Macromolecules*
27. S. Mendez, J. G. Curro, M. Puetz, D. Bedrov, and G. D. Smith, *J. Chem. Phys.*, 115, 5669 (2001)
28. J. D. McCoy, Y. Ye, and J. G. Curro, *J. Chem. Phys.*, 117, 2975 (2002)
29. S. Mendez, L. K. Ista, and G. P. Lopez, manuscript in preparation
30. D. L. Huber, R. P. Manginell, M. A. Samara, and B. C. Bunker, submitted to *Science*
31. A. B. Anderson and C. R. Robertson, *Biophys. J.*, 68, 2091 (1995)
32. M. Kleijn and W. Norde, *Hetero.Chem. Rev.*, 2, 157 (1995)

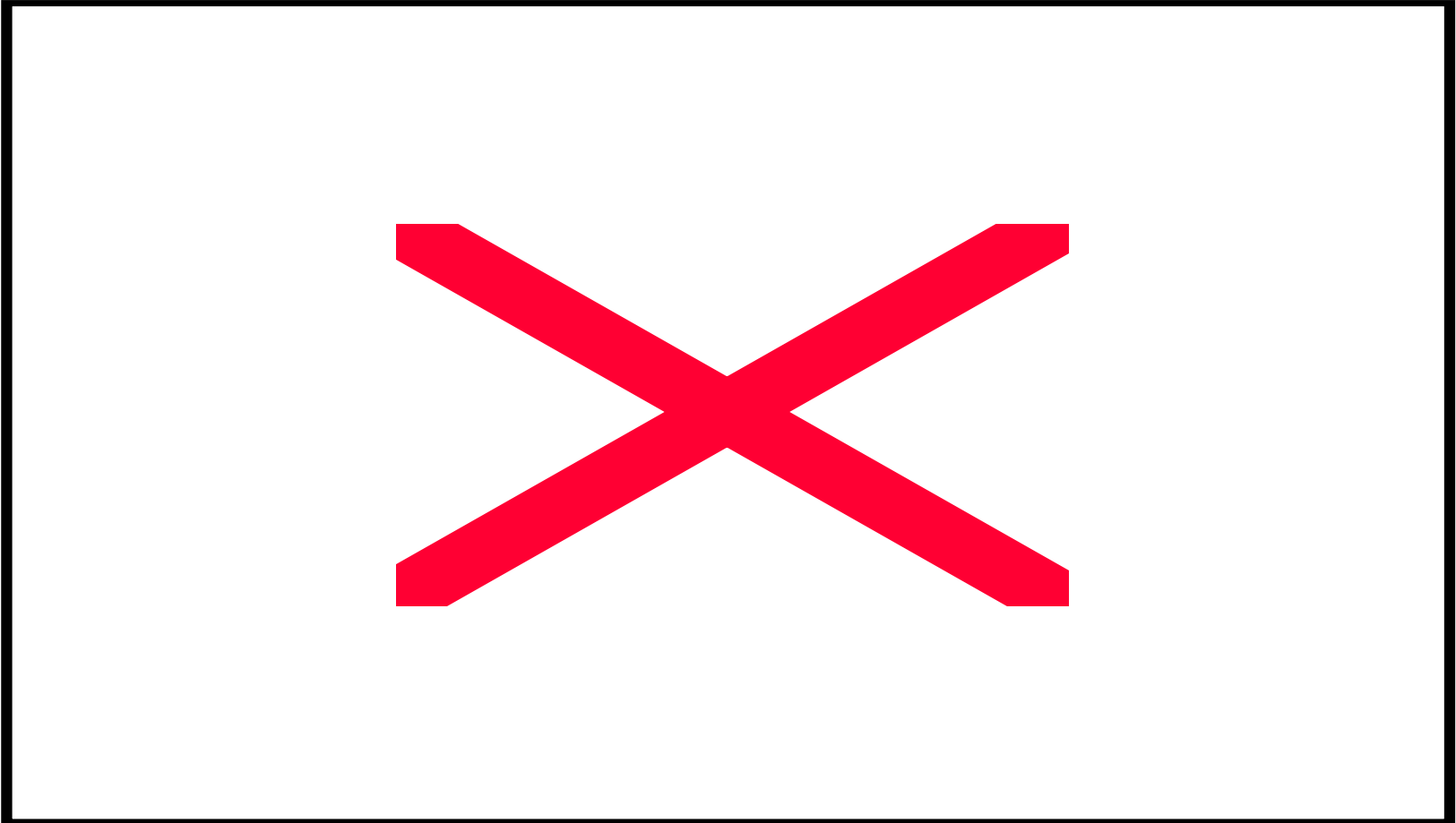


Fig. 1

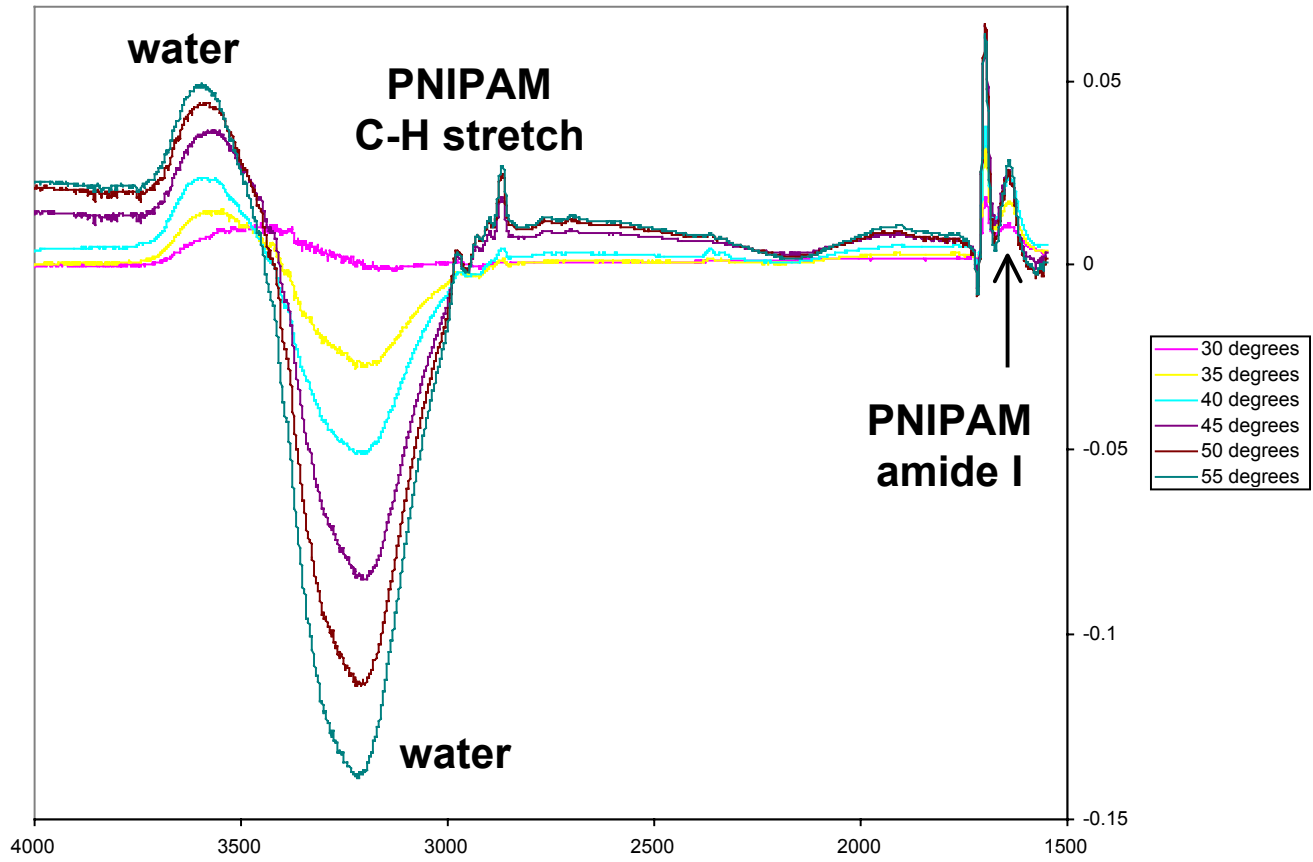


Fig. 2a

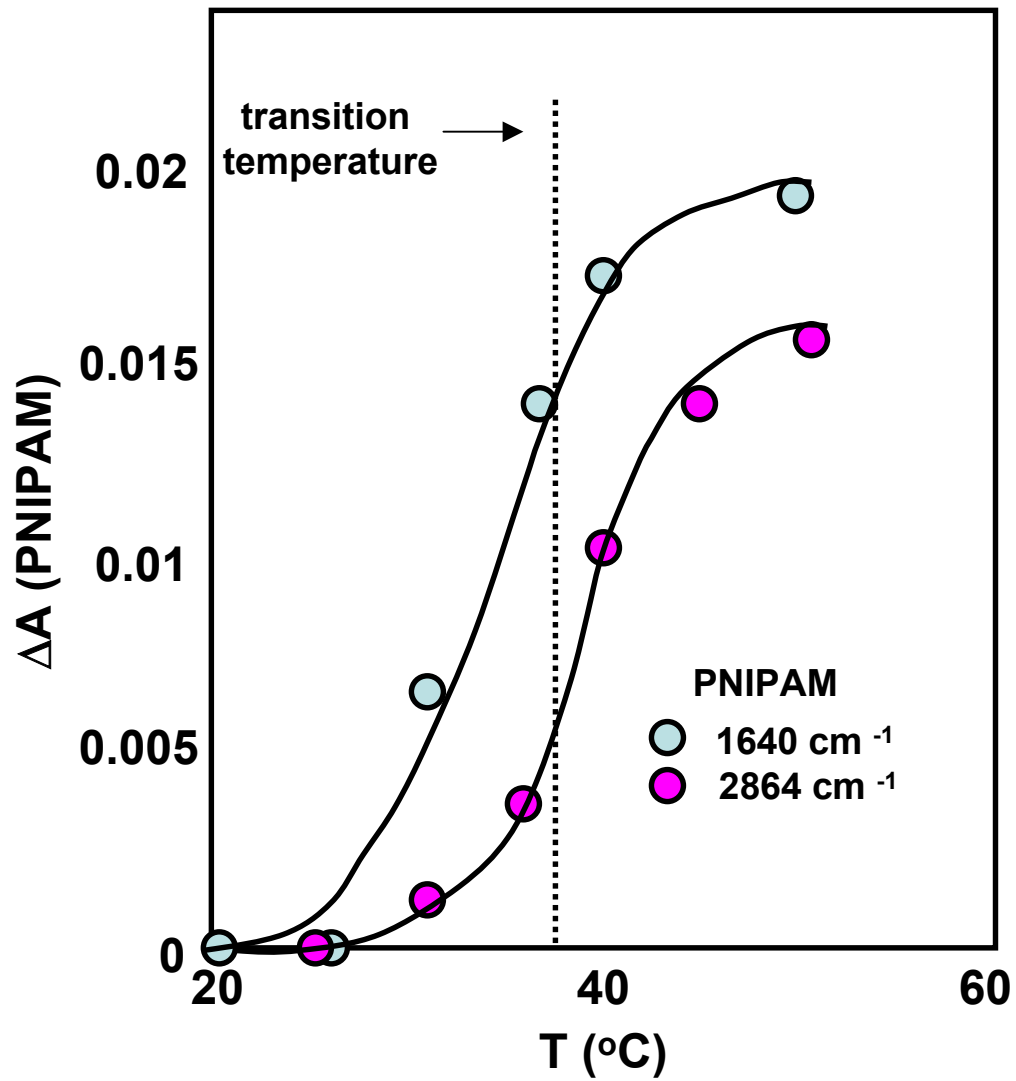
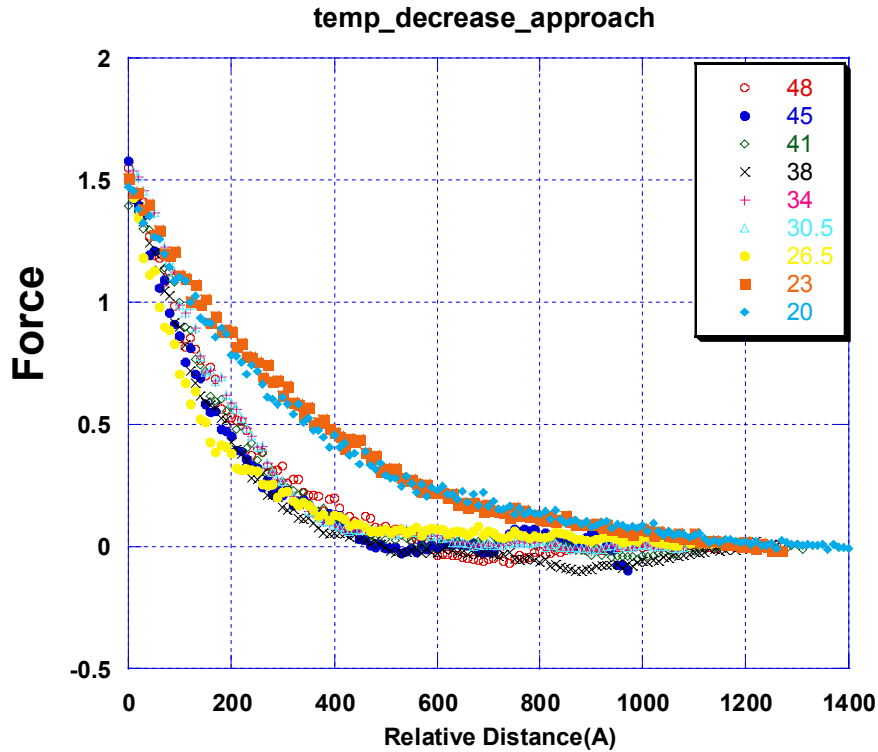


Fig. 2b

IFM on PNIPAM/Si under Water with ODTs coated Tip

-Decrease of Temperature from 48°C to 20 °C

Approach



Retraction

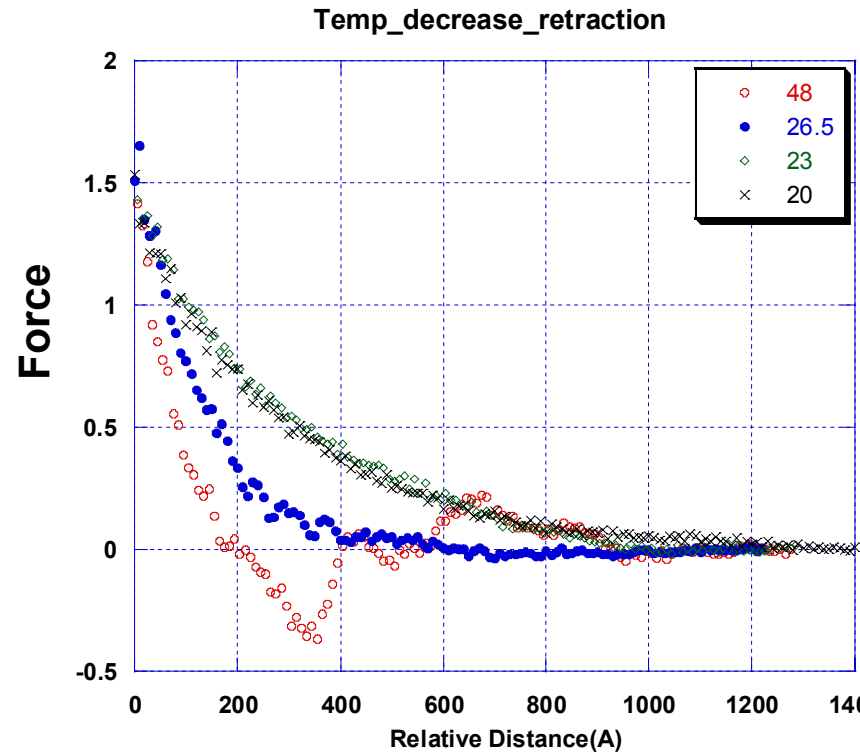


Fig. 3

Flory-Huggins χ Parameter

Cloud point curve for
PNIPAAM / Acetone Solution.
 $M_w/M_n = 3.64$, $M_v=249k$.

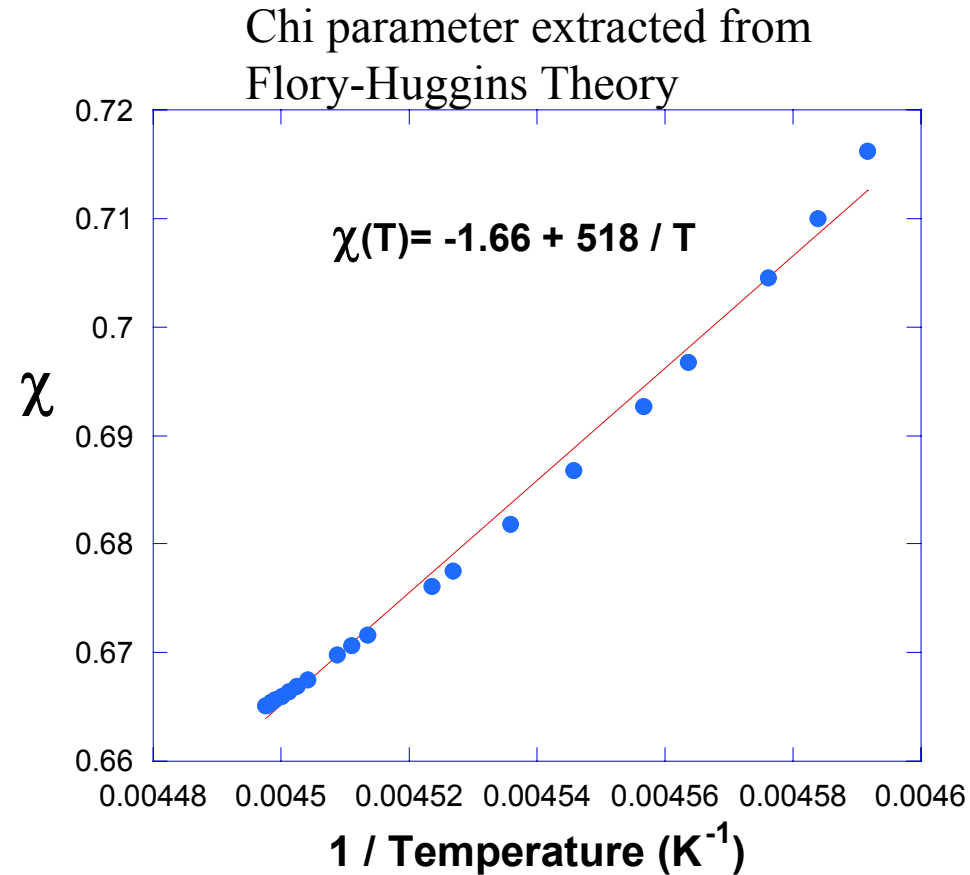
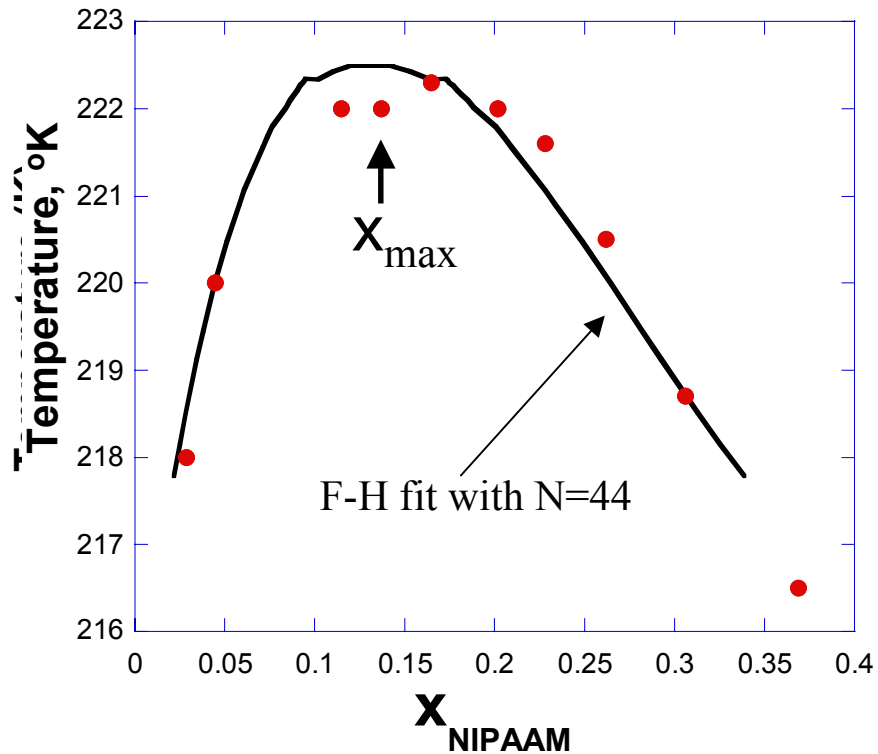
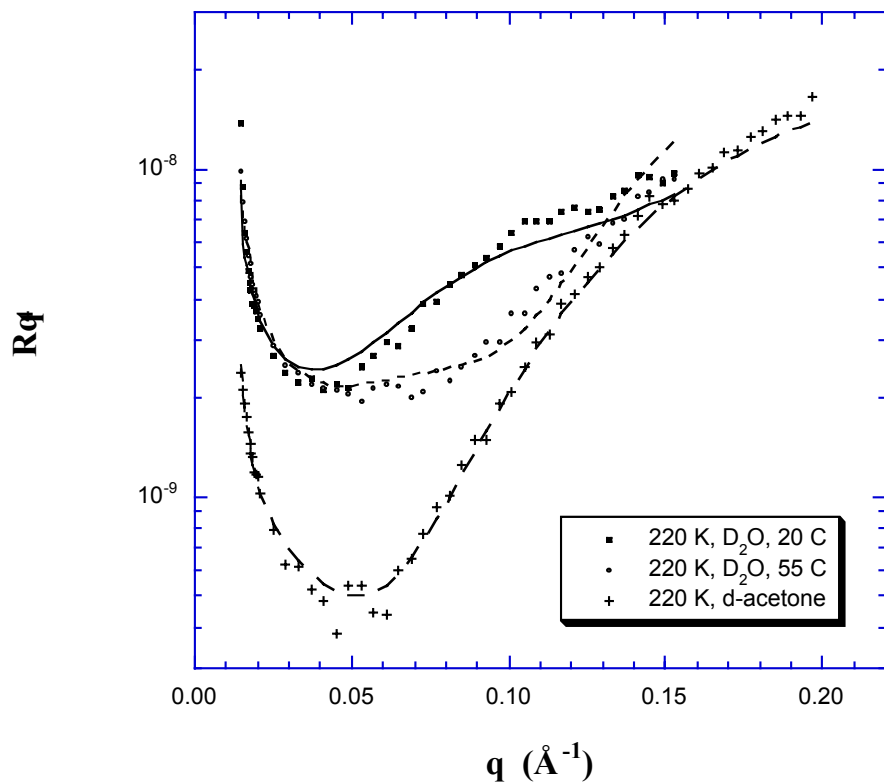


Fig. 4

(a)



(b)

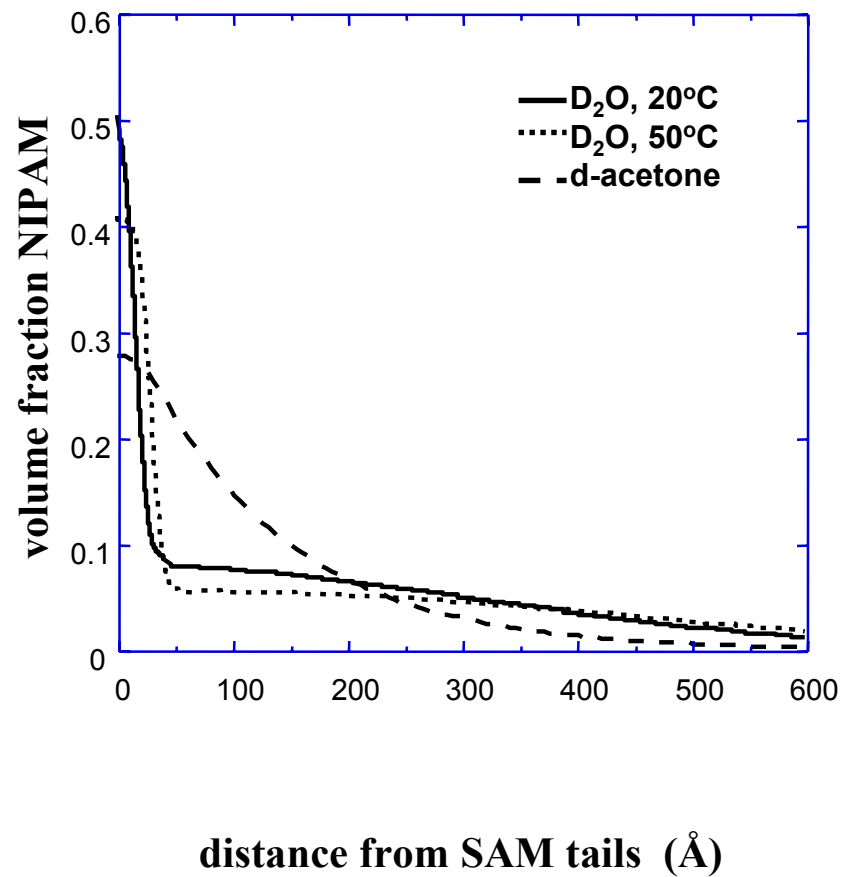
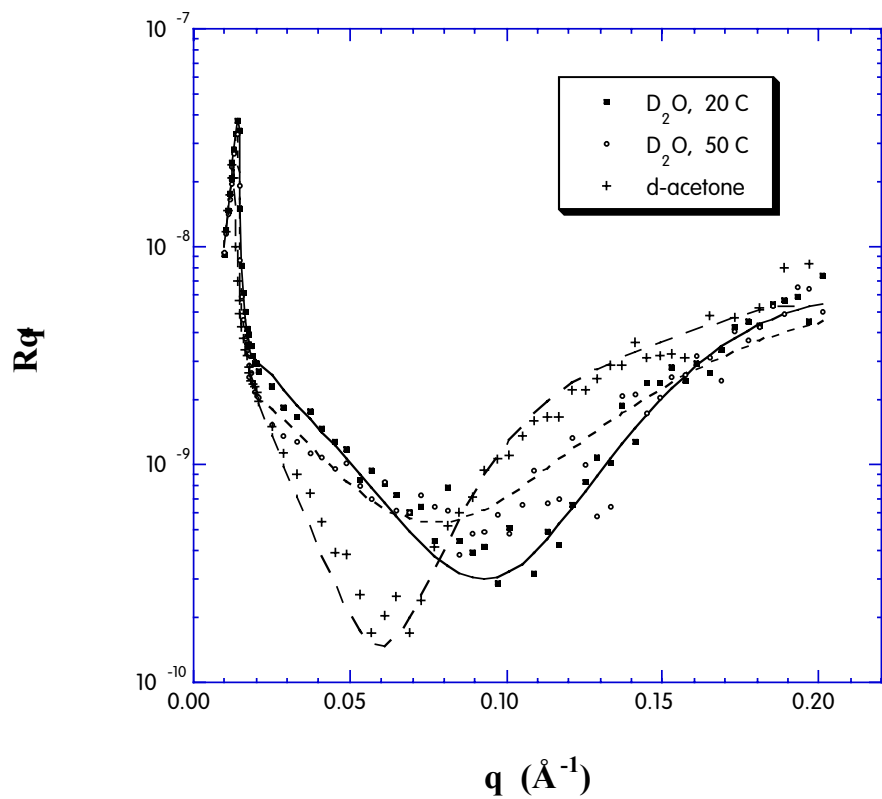


Fig. 5

(a)



(b)

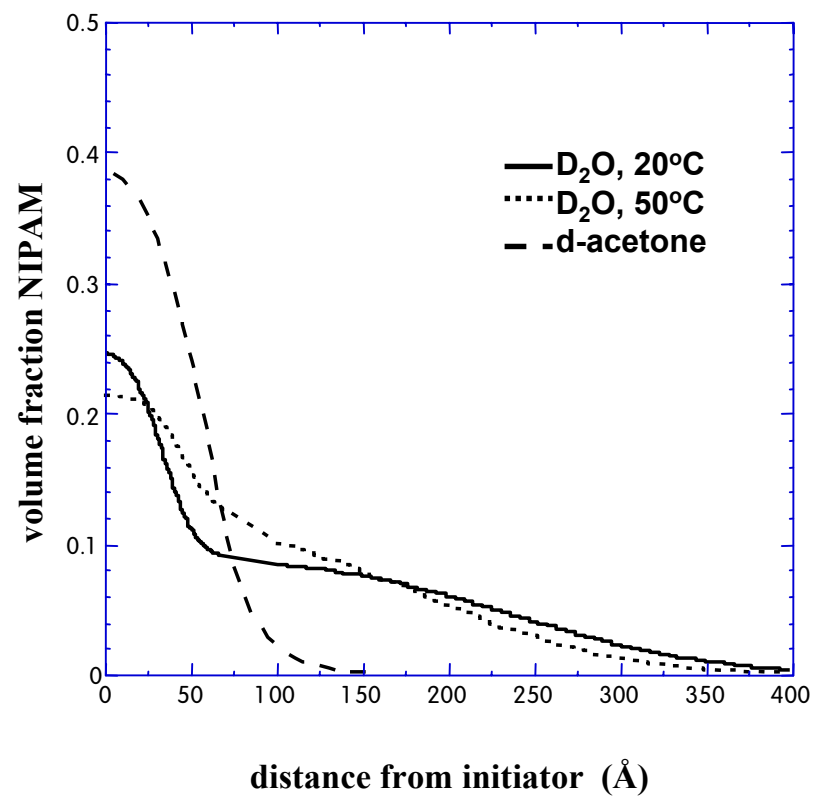


Fig. 6

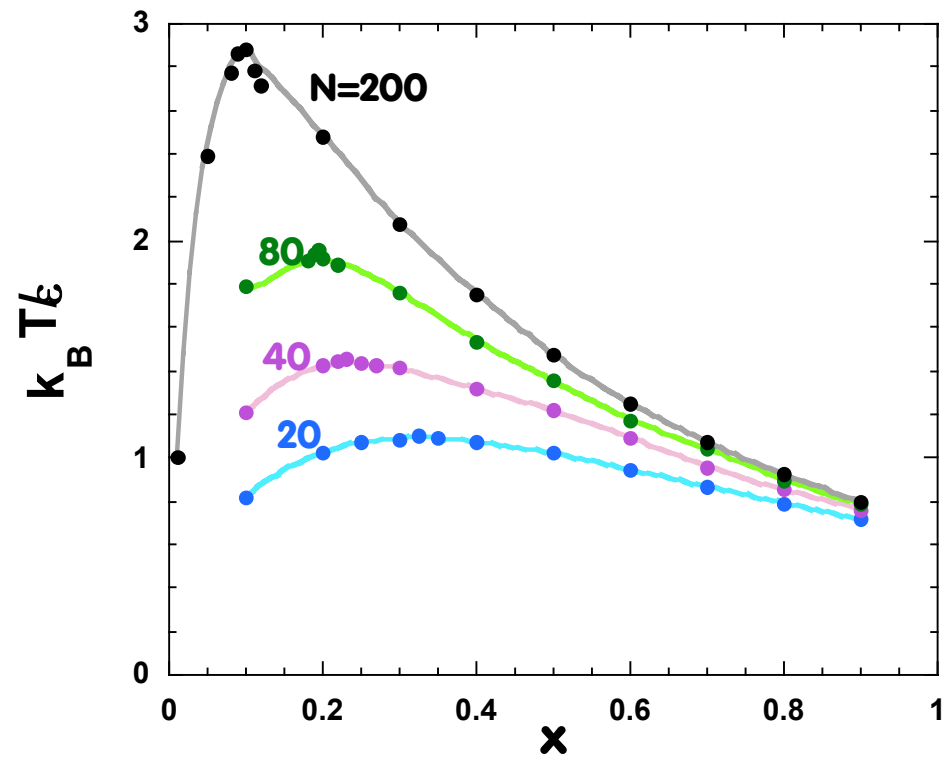


Fig. 7

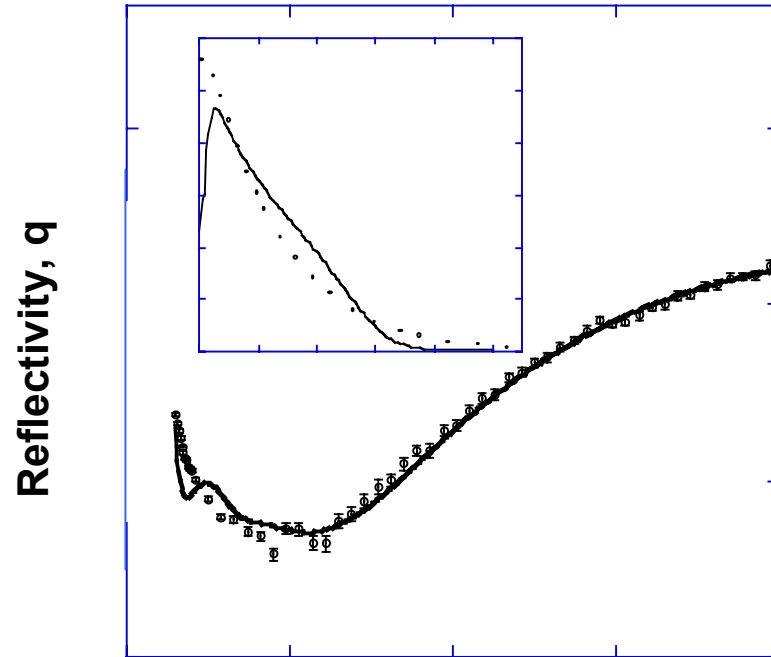
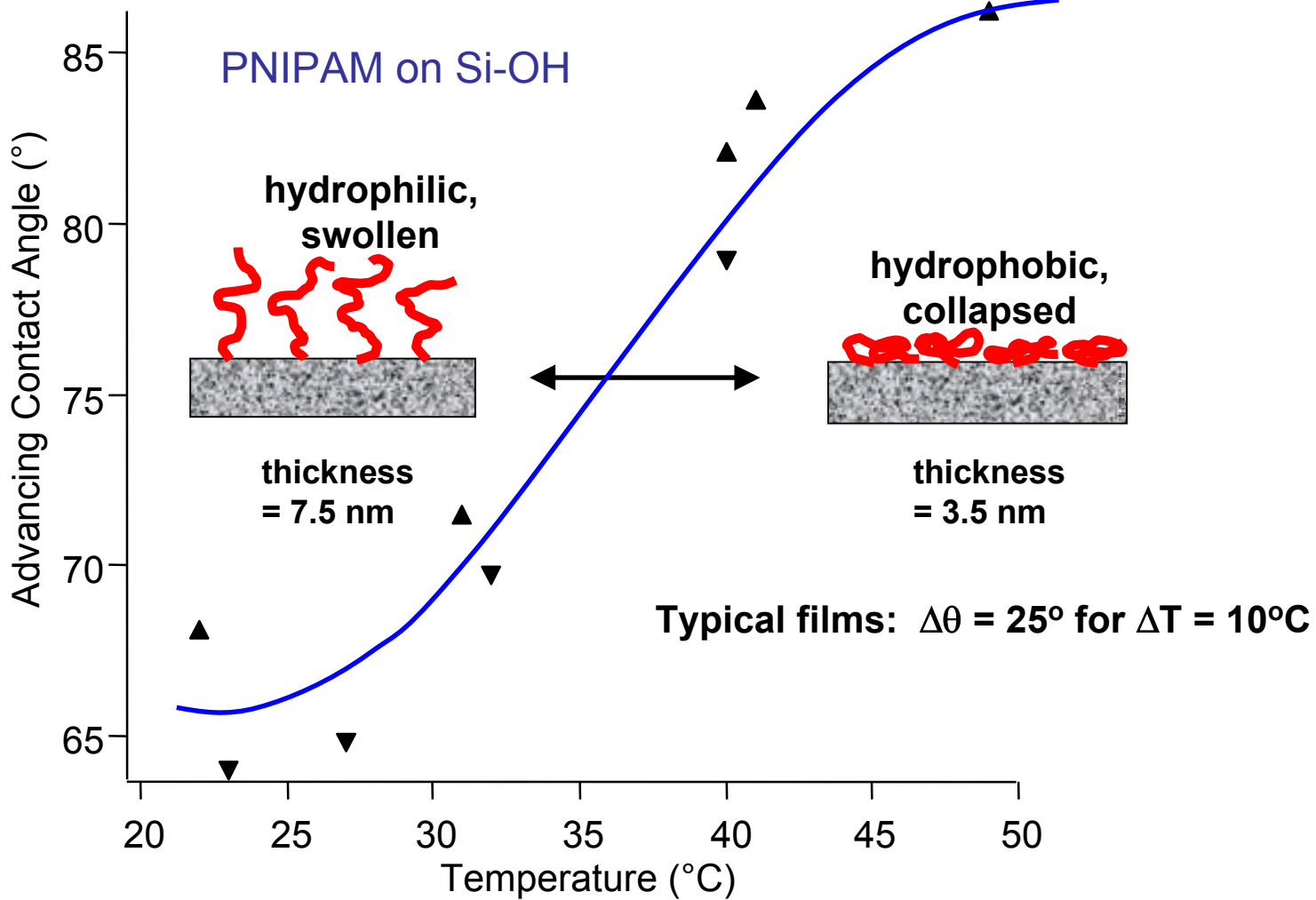


Fig. 8

Fig. 9



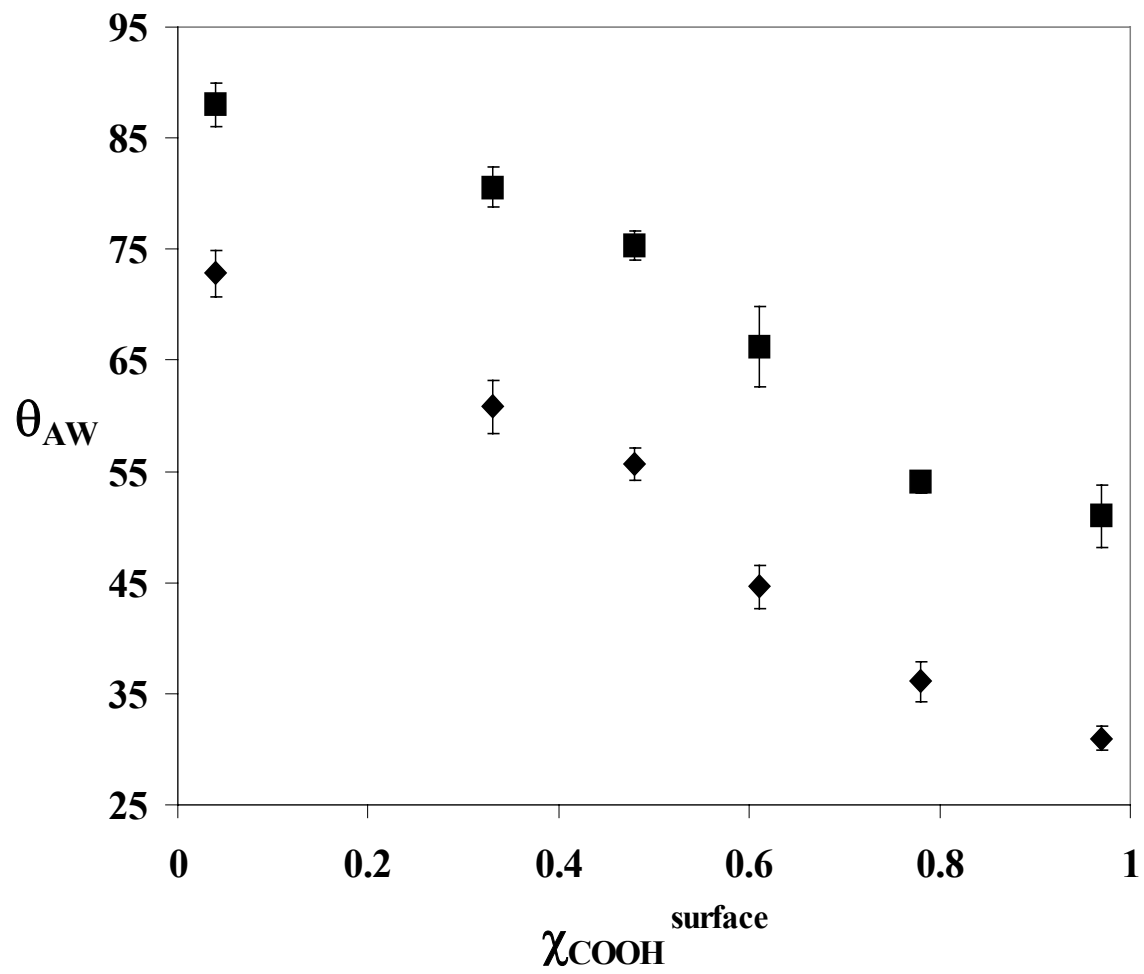


Fig. 10

Ellipsometry Results, Human Serum Albumin Adsorption

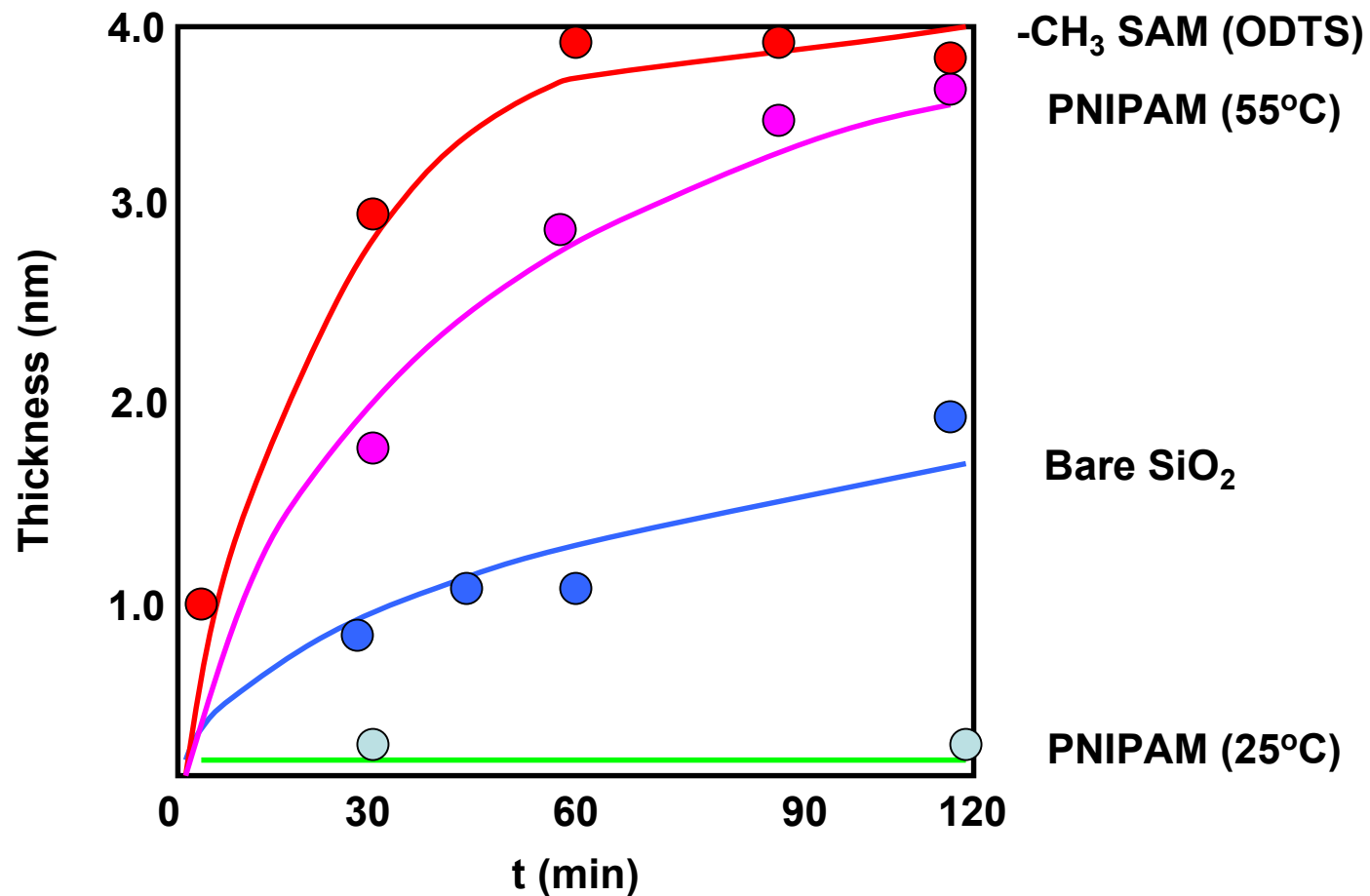
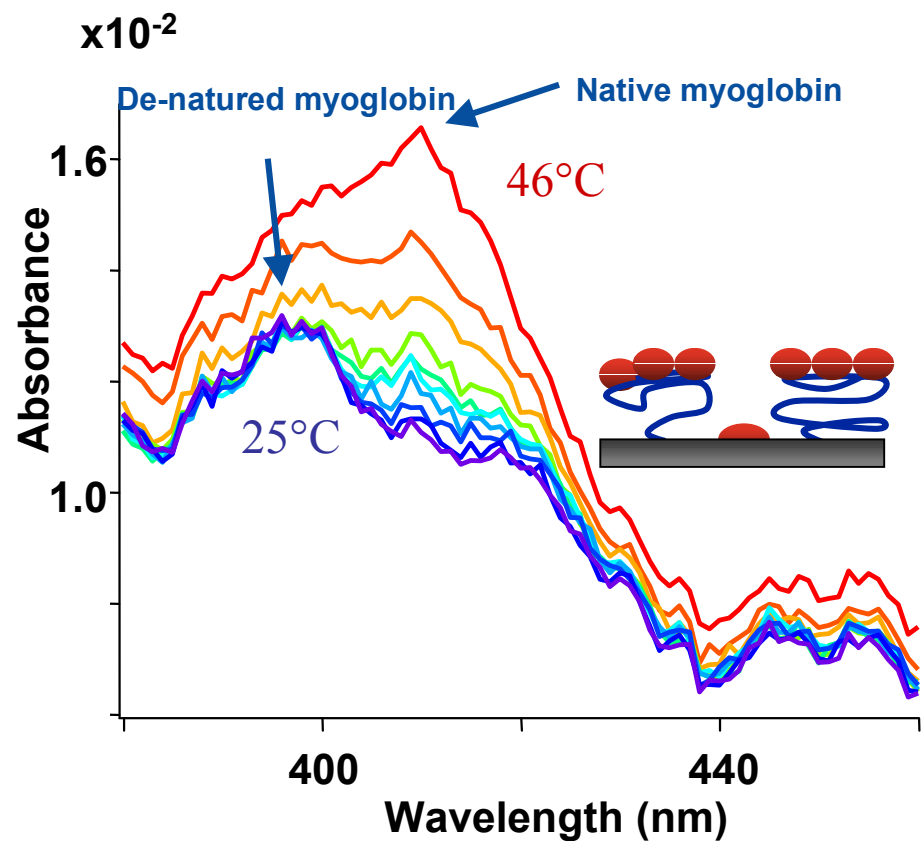


Fig. 11

(a) In Situ Radical Generation



(b) Chain Transfer to Surface

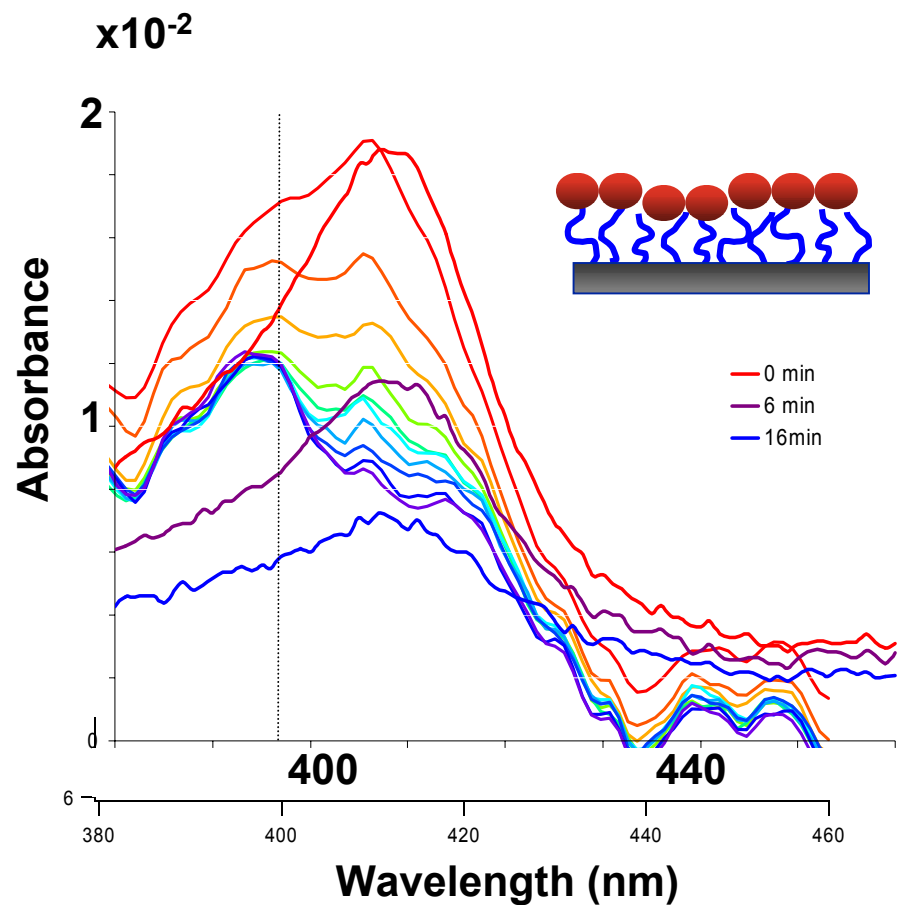
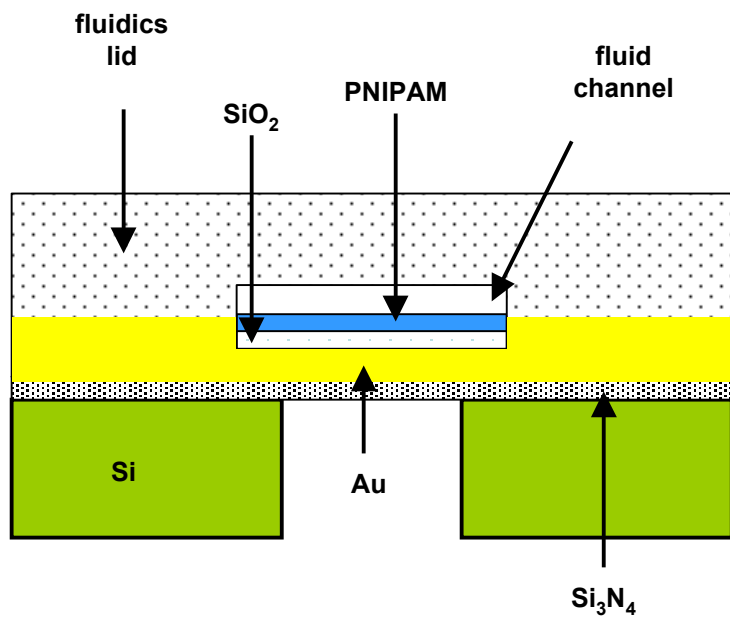
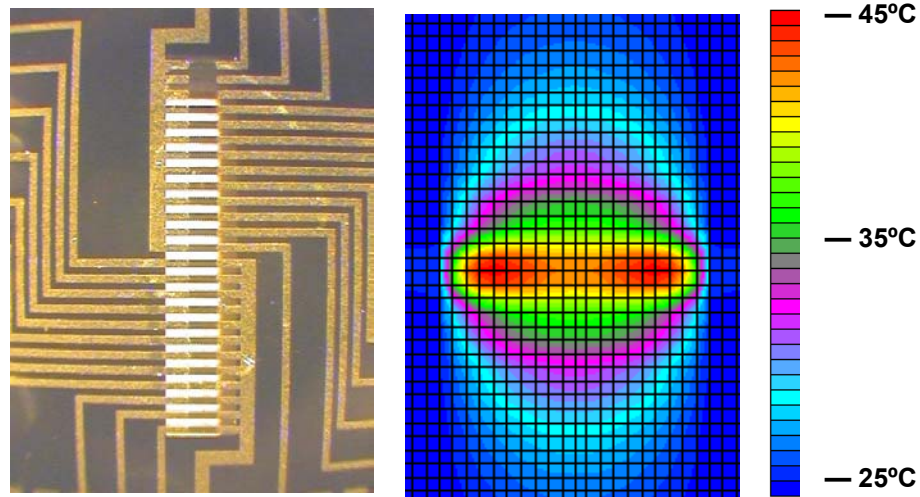


Fig. 12

a)



b)



c)

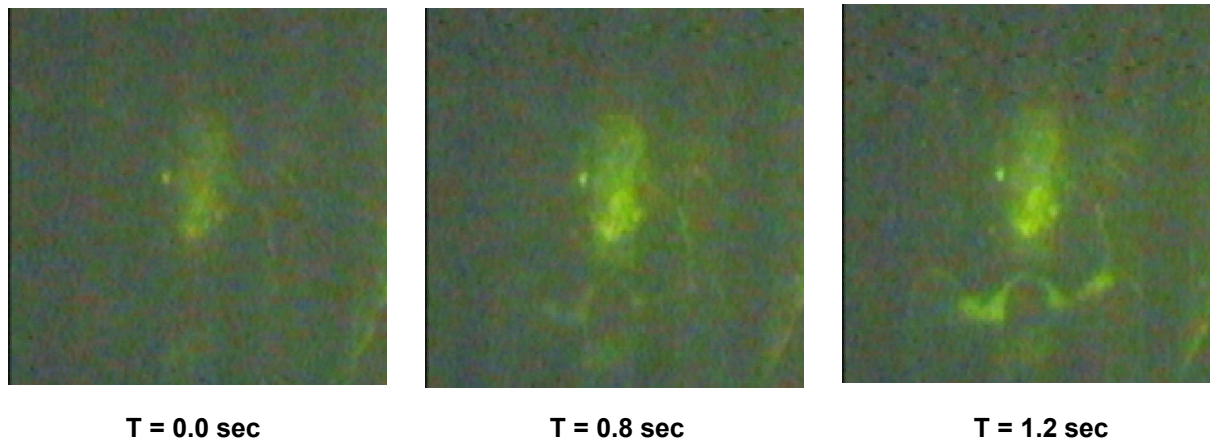


Fig. 13

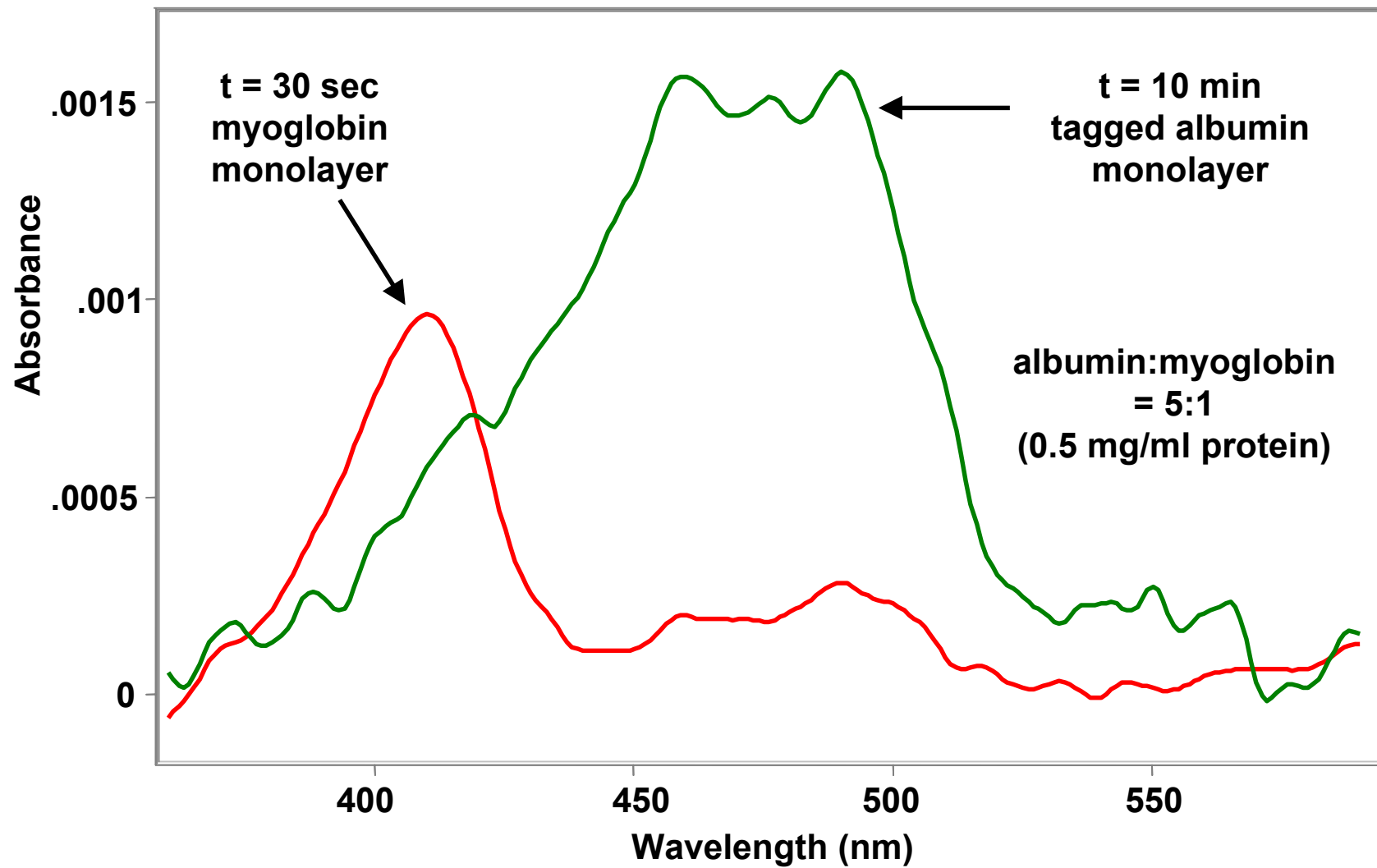


Fig. 14

Distribution:

2	MS1421	Dale L. Huber, 1122
6	1413	Bruce C. Bunker, 1141
1	1413	Paul V. Dressendorfer, 1141
3	1411	Michael S. Kent, 1851
4	1349	John G. Curro, 1834
3	0603	R. J. Manginell, 1764
1	9108	Central Technical Files, 8945-1
2	0899	Technical Library, 9616
1	0612	Review and Approval Desk, 9612 For DOE/OSTI
1	0188	LDRD Office, 1010